Title:

Methionine coordinates a hierarchically organized anabolic program enabling proliferation

Adhish S. Walvekar[1], Rajalakshmi Srinivasan[1], Ritu Gupta[1] and Sunil Laxman[1*]

[1] Institute for Stem Cell biology and Regenerative Medicine,

NCBS-TIFR campus, GKVK Post, Bellary Road, Bangalore 560065.

[*] Correspondence: sunil@instem.res.in

Keywords: methionine, S-adenosyl methionine, Gcn4, growth, pentose phosphate pathway, NADPH, reductive biosynthesis

Abstract

Methionine availability during overall amino acid limitation metabolically reprograms cells to support proliferation, the underlying basis for which remains unclear. Here, we investigate the organization and mechanism of this methionine mediated anabolic program, using yeast. Combining comparative transcriptome analysis, biochemical and metabolic flux based approaches, we discover that methionine, predominantly through Gcn4p, can rewire metabolic outputs by controlling specific regulatory nodes. Methionine increases the activity of three key nodes: the pentose phosphate pathway coupled with reductive biosynthetic capacity, and overall transamination capacity, including the synthesis of glutamate/glutamine. These processes allow the completion of subsequent rate-limiting reactions in the synthesis of costly amino acids, and nucleotides, which are also induced in a methionine dependent manner. This thereby results in a biochemical cascade establishing an overall anabolic program. Thus, methionine switches cells to anabolism, co-opting a "starvation stress response" regulator, Gcn4p, to achieve this. This suggests a hierarchical metabolic framework explaining how methionine mediates an anabolic switch.

Introduction

Cell growth is expensive, and is therefore tightly co-ordinated with the intrinsic cellular metabolic state. In general, the enormous metabolic costs incurred during growth and proliferation come from two well-studied phenomena. First, to successfully complete division, a cell makes substantial metabolic investments, in order to replicate its genome, and synthesize building blocks like amino acids, lipids, nucleotides, and other macromolecules (Nelson, DL; Cox, 2017). Second, the process of protein synthesis required for growth itself consumes large amounts of energy (Warner, 1999; Warner *et al*, 2001), as the translational

output of cells increases (Jorgensen & Tyers, 2004). Understanding such changes in cellular metabolic state coupled to global biosynthetic outputs, in the context of commitments to cell growth and proliferation are now the focus of several studies (Broach, 2012; Ljungdahl & Daignan-Fornier, 2012; Dechant & Peter, 2008; Brauer *et al*, 2008; Boer *et al*, 2010). For example, one context where there is intense interest in understanding metabolic alterations enabling growth is in cancers, where phenomena ranging from the Warburg effect (Warburg, 1956; Heiden *et al*, 2009), to the identification of the biosynthetic and metabolic requirements for cell growth (DeBerardinis *et al*, 2008; Tong *et al*, 2009; Heiden *et al*, 2009) are studied. Yet, given the overall complexity of metabolic rewiring, understanding how specific, "sentinel" metabolites can function as growth signals, and identifying the core, necessary steps by which such metabolites can rewire cells to an anabolic state, has been challenging.

However, simple, tractable cellular models can be used to dissect and deconvolute such complex phenomena. Studies using *Saccharomyces cerevisiae* have been particularly instrumental in identifying dedicated, conserved strategies utilized by eukaryotic cells to integrate metabolic state with growth (Gray *et al*, 2004; Cai *et al*, 2011; Slavov & Botstein, 2011; Ye *et al*, 2017; Brauer *et al*, 2008; Boer *et al*, 2010; Broach, 2012; Ljungdahl & Daignan-Fornier, 2012; Xu *et al*, 2013; Mulleder *et al*, 2016). In such reductive studies using yeast, preferred carbon or nitrogen sources are typically limited (thereby slowing down overall growth). Subsequently, specific factors are reintroduced individually or in combination. This thereby reconstitutes minimal components required for reprogramming cells to an anabolic state, and allows the precise identification of necessary components, or dissection of mechanistic events. Such approaches have discovered novel nutrient sensing systems, and mechanisms by which growth outputs are controlled by the build-up and utilization of specific metabolites (Boer *et al*, 2008; Tu *et al*, 2007; Slavov & Botstein, 2013;

61 Xu *et al*, 2013; Klosinska *et al*, 2011; Laxman & Tu, 2010; Sutter *et al*, 2013; Laxman *et al*,
62 2013; Tu *et al*, 2005; Brauer *et al*, 2008; Boer *et al*, 2010; Cai *et al*, 2011; Ye *et al*, 2017).

63 Interestingly, some amino acids can directly function as anabolic signals, potently
64 activating growth pathways independent of their roles as nitrogen or carbon sources. For
65 example, leucine and glutamine activate the TOR pathway directly (González & Hall, 2017;
66 Wolfson & Sabatini, 2017). In this context, studies from diverse organisms, observed over
67 many decades suggest that methionine is a strong growth signal, or "growth metabolite"
68 (Troen *et al*, 2007; Lee *et al*, 2016, 2014; Cavuoto & Fenech, 2012; Breillout *et al*, 1990;
69 Sugimura *et al*, 1959; Gu *et al*, 2017; Sutter *et al*, 2013). The most direct evidence for
70 methionine as a growth signal come from recent studies in yeast. When *S. cerevisiae* are
71 shifted from complex, amino acid replete medium with lactate as the carbon source, to a
72 minimal medium with the same carbon source, the addition of methionine alone (likely
73 through its metabolite S-adenosylmethionine (SAM)), strongly promotes growth and
74 proliferation (Wu & Tu, 2011; Laxman *et al*, 2014a; Sutter *et al*, 2013; Laxman *et al*, 2013;
75 Ye *et al*, 2017). Thus, even during otherwise overall nutrient limitation, methionine can
76 induce proliferation. Despite these advances, two fundamental, related questions regarding
77 methionine as a growth signal remain unanswered. First, what is the biochemical logic of the
78 methionine mediated anabolic program (i.e. how does methionine result in an anabolic
79 reporgramming)? Second, what is the mechanism by which methionine mediates this
80 anabolic rewiring, even in overall amino acid limiting conditions? We address these related
81 questions in this study.

82 Here, using a minimal, reconstitutive system in yeast, and a biochemical first-
83 principles approach, we uncover how methionine uniquely rewires cells to an anabolic state,
84 even in otherwise amino acid limited conditions. We find that methionine activates very
85 specific metabolic nodes in order to mediate this anabolic reprogramming. When these nodes

are coincidently activated, they further induce a cascade of dependent metabolic processes leading to the overall biosynthesis of “costly” amino acids and nucleotides. For appropriately executing this anabolic program and sustaining proliferation, cells unexpectedly co-opt Gcn4p, a mediator of a nutrient stress/survival response. Collectively, these results position methionine at the apex of an overall anabolic network, and provide an overarching metabolic logic to understand how methionine availability results in metabolic rewiring and controling cellular metabolic state.

Results

Methionine induced growth requires Gcn4p.

When wild-type, prototrophic yeast cells are shifted from a complex, amino acid rich medium with lactate as the sole carbon source (RM), to a synthetic minimal medium containing nitrogen base and lactate (MM), they show a significant lag phase and slower growth. Supplementation with all 20 standard amino acids restores growth after this nutrient downshift (Figure S1A) (Sutter *et al*, 2013; Laxman *et al*, 2014a). Importantly, methionine supplementation alone substantially increases growth (Figure 1A), comparable to (in our hands) or better than adding all eighteen other non-sulfur amino acids (nonSAAs) together (Sutter *et al*, 2013; Laxman *et al*, 2014a). Collectively, even during otherwise overall amino acid limitation, methionine availability can increase proliferation. Given that methionine is itself not a good "nutrient source" (i.e. a poor carbon or nitrogen source), and adding methionine alone would not create a nutrient replete medium, we wondered how methionine might mediate a switch to an anabolic state. This is a clear metabolic supply problem. We therefore thought that examining key growth/survival regulating nodes that are known to be altered during growth under nutrient stress (in the presence or absence of methionine) might serve as a good starting point from which to address this question. In the currently understood model for cellular responses to amino acid limitation (Figure 1B), the Gcn2p kinase is activated and phosphorylates eukaryotic initiation factor eIF2α. This results in global translational repression, but selective translation of *GCN4*, where the Gcn4 protein controls general amino acid biosynthesis (Figure 1B) (Hinnebusch, 2005). This process is well conserved across eukaryotes (Vattem & Wek, 2004). By monitoring the activity status of these steps within this model, and introducing methionine as a variable, we reasoned that clues might emerge that will lead us to the core metabolic phenomenon regulated by methionine. We therefore monitored outputs of responses during amino acid limitation

118 (illustrated in Figure 1B), to determine if any of these aspects were unusually altered in the
119 presence of methionine.

120 We first monitored global translational output by standard polysome profiling (Figure
121 1C). Expectedly, RM grown cells showed a 3:1 polysome: monosome ratio indicating robust
122 translation, and cells shifted to MM showed a drastic reduction in the polysome pool, and an
123 increased monosome peak (polysome:monosome ratio of ~1:1) (Figure 1C, Figure S1B).
124 Supplementation with either methionine, or all the nonSAAs combined, during the shift to
125 MM also showed an increase in the monosome pool, and a partial restoration of the polysome
126 levels resulting in a polysome: monosome ratio of ~1.7:1 (or ~1.3:1, for nonSAAs) (Figure
127 1C, Figure S1B), suggesting slightly increased translation due to methionine. We also
128 monitored the phosphorylation status of eIF2α (Figure 1D), and expectedly observed a
129 substantial increase in the phosphorylation levels of eIF2α after a RM to MM shift. However,
130 methionine supplementation only marginally reduced the levels of phosphorylated eIF2α, and
131 levels of phosphorylation remained high (Figure 1D). Collectively, the phosphorylation status
132 of the eIF2α, and the results obtained with polysome profiling, suggest that methionine has a
133 modest impact on global translation during amino acid limited growth, but the cells continue
134 to appear "nutrient stressed", while showing increased proliferation. These observations were
135 largely in line with expected outcomes.

136 We next monitored the amounts of endogenous Gcn4p (chromosomally tagged with a
137 C-terminal HA epitope) after a shift to MM, with and without supplementation of different
138 amino acids, expecting a decrease in Gcn4p amounts upon the addition of methionine.
139 Surprisingly, Gcn4p accumulated substantially upon methionine supplementation, compared
140 to MM, or supplementing all 18 other nonSAAs (Figure 1E). This was independently
141 confirmed using immunofluorescence based experiments (Figure S1C). We therefore asked
142 whether Gcn4p was necessary for the increased growth upon methionine supplementation.

Figure 1

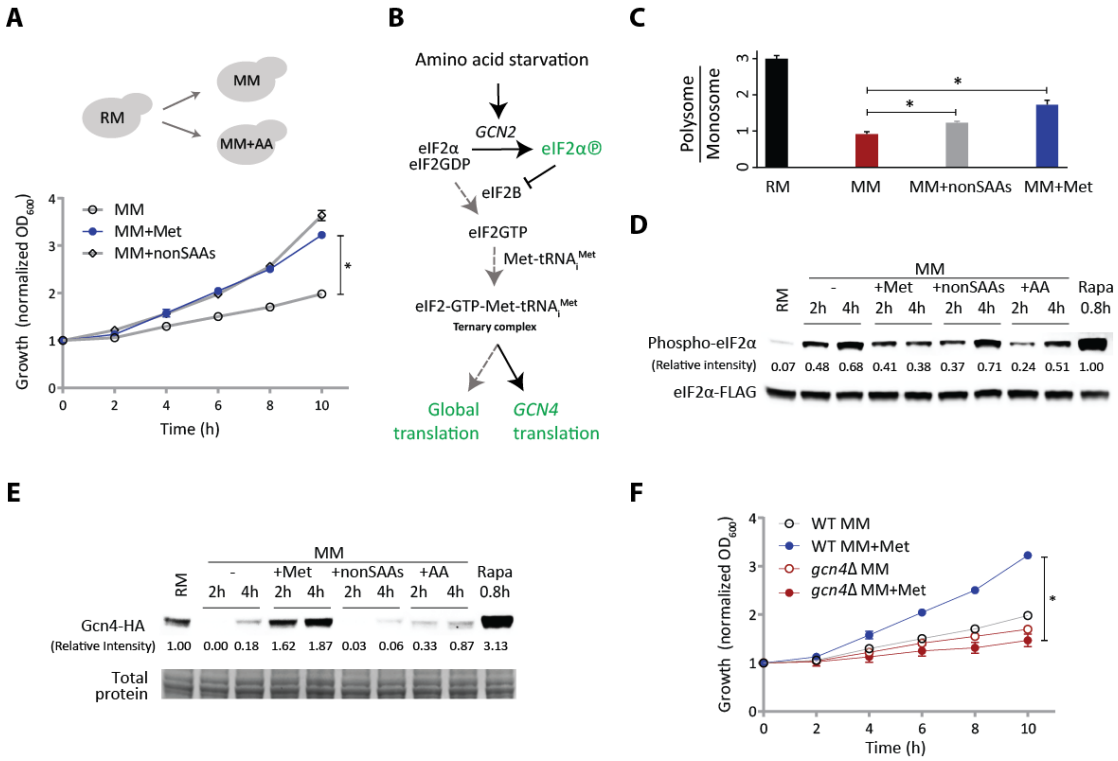

Figure 1: Methionine induced growth requires Gcn4p.

A) Methionine and growth during amino acid limitation. Shown are growth profiles of WT cells grown in RM and shifted to MM with or without the indicated amino acid supplements (2 mM each; nonSAAs indicates all the non-sulfur amino acids except tyrosine). The growth profile with methionine is in blue. Also see Figure S1A.

B) The current model explaining cellular responses to amino acid starvation. Amino acid starvation activates the Gcn2p kinase, leading to decreased levels of the ternary complex. The key outputs indicating amino acid starvation (highlighted in green) are increased phosphorylation of eIF2α, global translational repression, and induced Gcn4p translation.

C) Global translational repression is moderately rescued by methionine. WT cells were grown to mid-log phase in RM and shifted to MM, MM plus methionine or MM plus nonSAAs for two hours. The cells were treated with cycloheximide for 15 min before harvesting and polysome pool was fractionated on sucrose gradients using ultracentrifugation. The polysome/monosome ratio for the corresponding samples is shown. Also see Figure S1B.

D) Methionine and eIF2α phosphorylation. Yeast cells grown in RM were shifted to the indicated media. The samples were analysed for phosphorylation status of eIF2α (Sui2p in yeast) by Western blot. Rapamycin (100 nM) treated cells served as a positive control. WT cells expressing FLAG-tagged eIF2α were used to monitor the protein abundance under identical conditions. A representative blot is shown.

E) Gcn4p amounts in the presence of methionine during amino acid limited growth. Gcn4p was detected by Western blotting of WT cells (expressing Gcn4p with an HA epitope, tagged at the endogenous locus) shifted from RM to MM, or MM supplemented with the indicated

combinations of amino acids. RM grown cells treated with rapamycin (100 nM) served as a positive control for Gcn4p induction. A representative blot is shown.

F) *gcn4Δ* cells and methionine-mediated growth. The WT and *gcn4Δ* strains were shifted from RM to MM with or without methionine supplementation and growth was monitored. Also see Figure S1D.

In all panels, data shows mean±SD values. $^{*}p < 0.05$.

143 Notably, the *gcn4Δ* cells did not show any increased growth in methionine supplemented
144 medium, but instead only grew comparably to WT cells in MM (Figure 1F). As controls, in
145 all other conditions (lacking methionine, or in RM) the growth of *gcn4Δ* cells was
146 indistinguishable from the WT cells (Figure S1D). Collectively, these data indicate that
147 Gcn4p is necessary uniquely for the methionine-mediated growth in these amino acid poor
148 conditions. Given the established role of Gcn4p as a regulator of metabolic homeostasis, this
149 suggested that methionine triggered a core transcriptional response which potentially could
150 be deciphered, and a key component of this response (related to metabolism) might be
151 mediated by the Gcn4p transcription factor. Thus, we reasoned that dissecting the
152 methionine-mediated overall transcriptional response might provide insight into the anabolic
153 reprogramming mediated by methionine, and allow the elucidation of a core metabolic
154 response that drives proliferation.

155

156 **Methionine induces a transcriptional remodelling program driving key anabolic nodes.**

157 These data raise two questions: (i) what is the underlying logic of the anabolic
158 rewiring mediated by methionine?, and (ii) what is the contribution of Gcn4p towards this
159 anabolic state switch? We started with a comparative RNA-seq approach in order to address
160 aspects of both questions. In this section we first address how methionine reprograms cells
161 into an anabolic state, focusing on relatively early transcriptional events (before the overall
162 proliferation is observed). We performed RNA-seq analysis on distinct sample sets of wild-
163 type cells- (i) RM grown, or cells shifted to (ii) MM for 2h, (iii) MM+Met for 2h (Met set),
164 and (iv) MM+nonSAAs for 2h. Transcript reads from the biological replicates showed
165 exceptional correlation across all conditions (Pearson correlation coefficient, $R \geq 0.99$) (Figure
166 S2). Setting a stringent cut-off, we only considered differentially expressed genes with $\geq \log_2$

167 1.5 fold changes (i.e. ~2.8 fold change), and a p-value cut-off $<10^{-4}$ for further analysis. We
168 first compared global transcription trends in WT cells growing in RM, MM+Met or
169 MM+nonSAAs to MM, with the focus being what happens when methionine is the sole
170 variable. We examined overall global gene expression trends in these conditions (compared
171 to MM), looking at the distribution of the most induced or downregulated genes (Figure 2A,
172 Figure S3). When we compared the global gene expression trends (broad trends of up- or
173 down- regulated genes) exhibited by cells in MM+Met to those in other conditions, the
174 MM+Met gene expression signature was more greatly resembled cells in RM, than the cells
175 in MM+nonSAAs (which were nearly indistinguishable from MM) (Figure 2A, Figure S3
176 and S4). This suggests that methionine alone is perceived by cells as a stronger anabolic cue
177 than all non-sulfur amino acids combined, and is sufficient to switch cells into a
178 transcriptional state resembling that of rapidly proliferating cells in complex, amino acid rich
179 media.

180 We next more closely examined the transcriptional response unique to methionine, by
181 comparing transcriptomes of cells growing in MM vs MM+Met (the only variable being
182 methionine). This comparison identified 372 genes, of which 262 genes were upregulated in
183 the +Met set (Figure 2B, Figure S4, Supplementary file E1). Using gene ontology (GO),
184 these genes were grouped into related processes (Figure 2C, Figure S5A, Supplementary file
185 E2). We expectedly observed a substantial transcriptional response related to the core
186 translational machinery. Additionally, GO also grouped multiple induced genes into
187 categories that would fit generally under "nucleotide metabolism" (Figure 2C). GO broadly
188 fits these under "purine/pyrimidine" or "nucleobase and nucleotide metabolism", along with
189 the biosynthesis of secondary metabolites (Figure 2C). All of this would be entirely expected
190 for any cell in a "growth/proliferative" state, since proliferation relies on increased translation

Figure 2

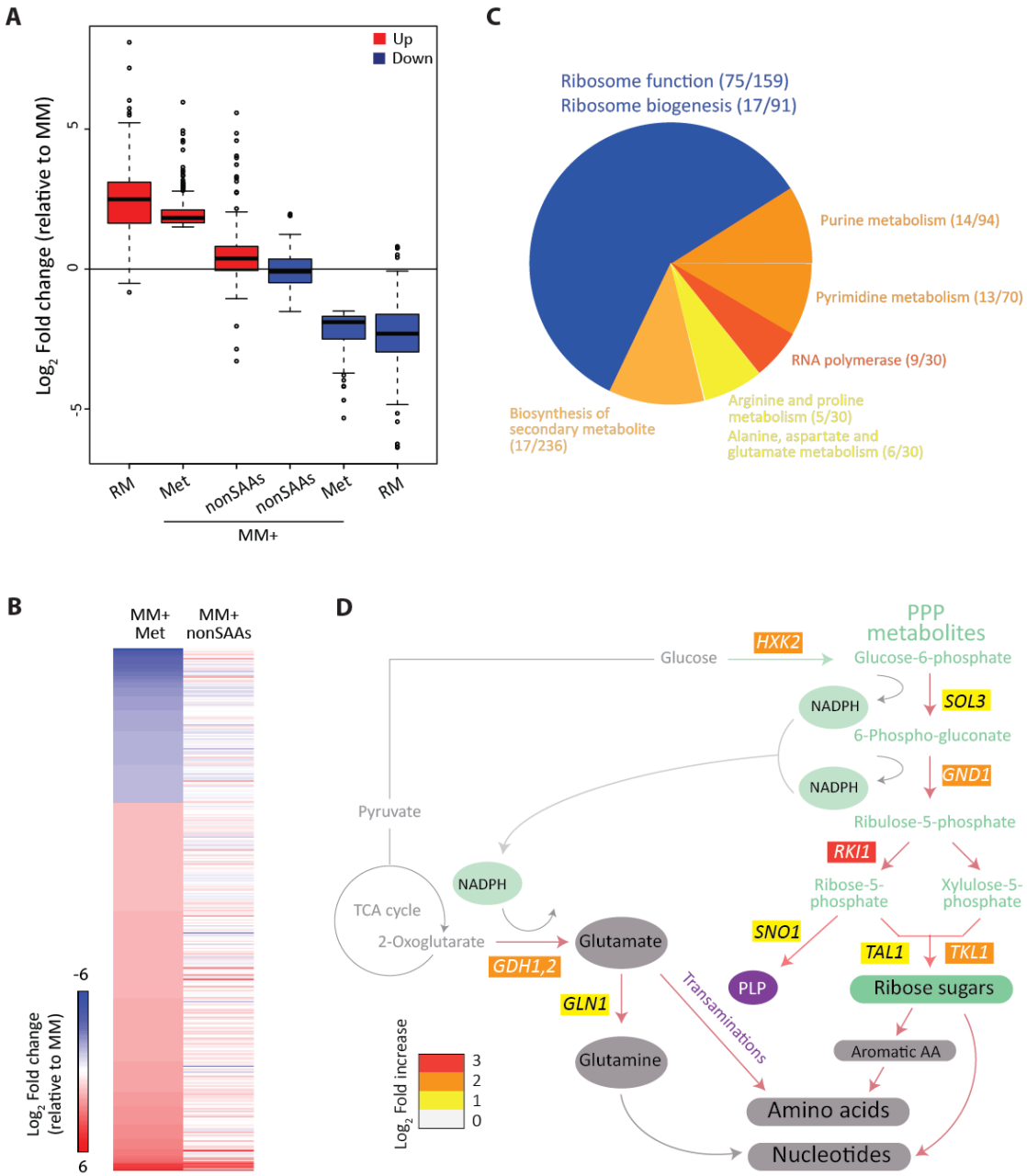

Figure 2: Methionine induces a transcriptional remodelling program driving key anabolic nodes.

A) Global trends of gene expression in RM and methionine supplemented MM. Boxplot shows gene expression levels of transcripts in WT cells grown in RM, or shifted to MM plus methionine, or MM plus nonSAAs in comparison to MM set.

B) Effect of methionine on a transcriptional program in cells. The heat map shows differentially expressed genes in MM plus methionine and MM plus nonSAAs compared to MM set.

C) GO analysis of the methionine-responsive genes. The pie-chart depicts the processes grouped by GO analysis for the up-regulated transcripts between MM plus methionine and

MM set. Numbers in the bracket indicate the number of genes from the query set/ total number of genes in the reference set for the given GO category.

D) Manual regrouping of the methionine responsive genes into relevant metabolic pathways, focusing on carbon metabolism and central metabolic processes. The pathway map includes individual genes in central carbon metabolism which are induced by methionine (indicating the fold-changes in gene expression). The arrows marked red indicate increased expression across the pathway.

191 and replication. Unsurprisingly therefore, the GO grouping showed a signature of a cell in a
192 "proliferative state".

193 However, this form of GO based grouping does not lend any insight into the
194 underlying metabolic logic or hiererchy of the methionine mediated anabolic response, and
195 only reveals the obvious readouts for growth. This is a limitation of using GO based analysis,
196 which builds groups by looking for enriched pathway terms (relying on multiple genes within
197 a pathway to be overrepresented). Contrastingly, for metabolic changes, entire metabolic
198 pathways need not be regulated. This is because most metabolic regulation happens by
199 controlling only key nodes or "rate-limiting steps" in metabolism (Nelson, DL; Cox, 2017).
200 We therefore rebuilt connections from biochemical first principles, in order to examine if
201 methionine only affected unique metabolic nodes, in order to attempt to put together a logical
202 hierarchy of metabolic responses being set-up. In this reconstruction, we particularly
203 emphasized: (i) whether the protein encoded by the gene regulated a "bottleneck" metabolic
204 step, and (ii) whether this biochemical step, and its subsequent product, was critical for
205 multiple other biosynthetic reactions. These nodes will not necessarily be picked up in GO
206 enrichments, particularly if they are solitary, and entire metabolic pathways are not
207 transcriptionally upregulated. However, they may in fact be central to understanding the
208 metabolic state. Through this reconstruction, we compartmentalized the metabolic response
209 regulated by methionine into a group of key biochemical reaction nodes, which could explain
210 how a majority of the other metabolic processes are subsequently upregulated, as described
211 below.

212 Only a few genes involved in classical "central carbon/carbohydrate metabolism"
213 were upregulated in the presence of methionine, and strikingly none of them group to
214 glycolysis, the TCA cycle or gluconeogenesis (Figure 2D). However, the genes encoding
215 three key enzymes of the pentose phosphate pathway (PPP) (*GND1*, *RKI1* and *TKL1*), which

216 regulate four steps in the PPP, were highly induced in the presence of methionine (Figure
217 2D). Furthermore, two other genes (*SOL3* and *TAL1*), which control two other steps in the
218 PPP, were also induced by methionine (at just below the $\log_2$ 1.5 fold (~2.8 fold) cut-off limit
219 we had arbitrarily set) (Figure 2D). Gnd1p catalyzes the last step in the oxidative arm of the
220 PPP, generating NADPH and producing ribulose-5-phosphate. Most of the genes of the non-
221 oxidative arm of the PPP, which make ribose-5-phosphate and other critical intermediates,
222 are also upregulated (Figure 2D). Additionally, *HXK2*, encoding a hexokinase is highly
223 upregulated when methionine is present. While this is not even classified under the PPP by
224 GO grouping, this enzyme produces glucose-6-phosphate, which is the substrate for the first,
225 rate-limited step of the PPP, and so we included it under the PPP in our grouping (Figure
226 2D). Thus, only the PPP arm of carbon metabolism was induced by methionine. Second, we
227 noted that key regulator resulting in the formation of pyridoxal-5-phosphate or PLP (encoded
228 by *SNO1*), was induced (Figure 2D). PLP a central metabolite, which is required for all
229 transamination reactions (Nelson, DL; Cox, 2017). Third, transcripts of Gdh1p, which
230 regulates the key nitrogen assimilation reaction resulting in the formation of glutamate (and
231 *GLN1*, which is further required to make glutamine), was highly induced in methionine
232 (Figure 2D). This reaction itself requires NADPH (which is produced in the PPP, Figure 2D),
233 and importantly is also critical for the subsequent formation of all other amino acids, and
234 nucleotides (Figure 2D). Thus, this grouping suggested that methionine induced the PPP-
235 GDH-PLP nodes in metabolism. We hypothesized that this PPP-GDH-PLP node could be
236 central for all the subsequent, downstream anabolic outputs.

237

238 **Methionine sets-up a hierarchical anabolic response**

239 We therefore inspected the other up-regulated genes that could be grouped broadly
240 under "amino acid biosynthesis", "nucleotide synthesis", and
241 "oxidoreduction/transamination" categories, particularly focusing on the substrates or co-
242 factors required for their function. Notably, only a few genes in each of these pathways were
243 induced, despite most of these pathways being multi-step, multi-enzyme pathways. However,
244 when organized by their biochemical requirements, essentially all enzymes encoded by this
245 set of upregulated genes utilized either a PPP intermediate/product, and/or NADPH, and/or
246 glutamate/glutamine, or combinations of all of these, i.e. products coming from the PPP-
247 GDH-PLP nodes (Figure 3A). We next more closely examined the steps in the respective
248 biosynthetic pathways that these genes regulated (coming from Figure 3A). Here, we further
249 categorized all steps in the amino acid biosynthesis pathway as either the rate-
250 limiting/initiation step and/or final step in the production of that amino acid, and organized
251 them based on the use of costly and complex precursors or cofactors (Figure 3B). Strikingly,
252 we observed that the methionine induced genes (few in number) in these pathways regulated
253 only the most critical, rate-limiting or costly steps in amino acid biosynthesis (p-value of
254 $3.8e^{-09}$, Fisher's exact test), but had little or no significant role in regulating the multiple other
255 genes in the pathway that encode enzymes for the other, inexpensive steps (Figure 3B).
256 Finally, we note that these methionine-induced genes in the "amino acid biosynthesis" bin do
257 not just broadly represent all amino acid biosynthesis, but synthesize what are viewed as the
258 costliest amino acids to synthesize (Barton *et al*, 2010), namely the aromatic amino acids, the
259 branched-chain amino acids, and lysine, which is highly overrepresented in ribosomal and
260 core translational machinery proteins (Laxman *et al*, 2013).

261 Similarly, nucleotide biosynthesis involves very large, multi-step pathways. The
262 methionine dependent, upregulated genes again encoded enzymes that control only specific
263 critical, limiting steps in nucleotide synthesis, and utilize glutamate/glutamine and/or

Figure 3

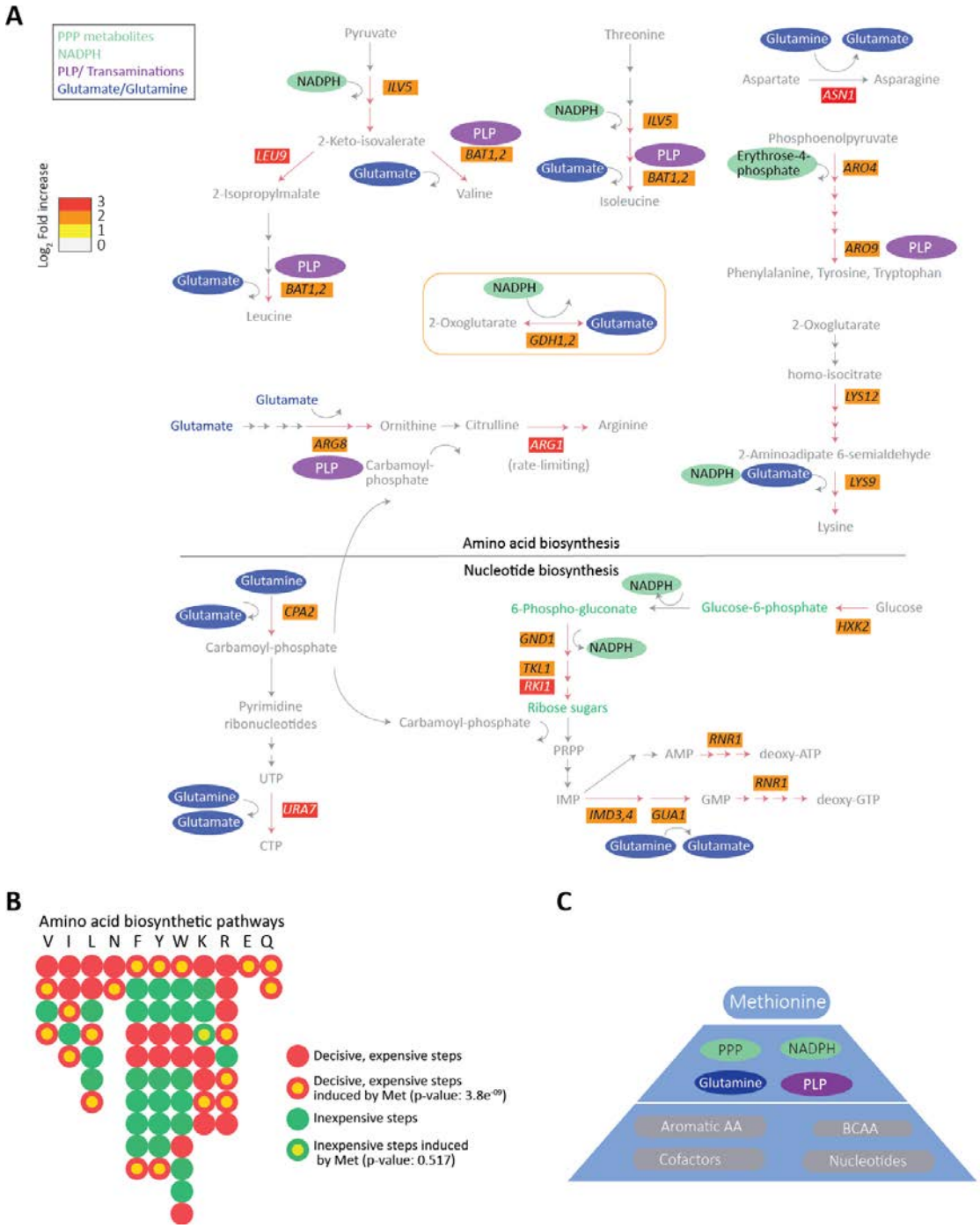

Figure 3: Methionine sets-up a hierarchical metabolic response leading to anabolism.

A) Regrouping of the methionine responsive genes in amino acid and nucleotide metabolism onto their respective pathways. The schematic shows the methionine-responsive genes in various amino acid and nucleotide biosynthesis pathways, along with their fold-changes in gene expression. The requirement of PPP metabolites, NADPH, PLP or glutamate/glutamine for the individual steps is mapped on to the schematic. The arrows marked red are the steps induced in the presence of methionine. Note that all these regulated steps use PPP intermediates, and/or NADPH, and/or PLP and/or glutamine/glutamate.

B) A bird's eye-view of the amino acid biosynthesis steps regulated by methionine. Each bead (or filled circle) represents a step in the pathway (prepared according to the individual amino acid pathways shown at https://pathway.yeastgenome.org/.) A step is considered expensive (marked red) when it is either the entry or the final or involves ATP utilization or involves reduction. All the rest of the steps are considered inexpensive (marked green). Methionine responsive steps are shown with a yellow fill at the centre of the circle, for the given step. The p-value for methionine dependence of genes encoding the critical, rate-limiting or costly steps in amino acid = $3.8e^{-09}$, and for the other nodes, it is non-significant (Fisher's exact test).

C) A hierarchical organization of the methionine mediated anabolic remodelling. Methionine induces expression of genes in the PPP-GDH-PLP node, which provides precursors for the overall biosynthesis of amino acids and nucleotides.

264 NADPH, as well as pentose sugars from the PPP, i.e. the PPP-GDH-PLP nodes (Figure 3A).
265 Notably, *RNR1*, which encodes the key enzyme in converting ribonucleotides to
266 deoxyribonucleotides (and hence the critical hub for DNA synthesis), is strongly upregulated
267 upon methionine addition (Figure 3A). Separately, we expanded this analysis and compared
268 the methionine response to minimal medium supplemented with all other nonSAAs, and here
269 the overall metabolic grouping or organization remained unchanged (Figure S4), with
270 nonSAAs resembling MM. Finally, in MM+nonSAAs, the few highly induced genes
271 (compared to RM) function in methionine (and sulfur-amino acid) related biosynthesis or
272 salvage (Figure S5B, Supplementary file E1), and not additional reactions. This further
273 substantiates our overall observations for the role of methionine as an "anabolic signal".

274 Collectively, this comparative transcriptome analysis, done from a biochemical first
275 principles perspective, suggests not just a general anabolic remodelling due to methionine,
276 but a hierarchical metabolic organization induced by methionine (Figure 3C). In this putative
277 hierarchical organization, methionine induces genes regulating the PPP, key transamination
278 reactions, and the synthesis of glutamine/glutamate (the PPP-GDH-PLP node). These three
279 processes directly allow critical steps in synthesis of the costliest amino acids and
280 nucleotides. The key, limiting steps in these subsequent synthesis reactions are themselves
281 induced by methionine, collectively setting up a structured anabolic program (Figure 3C).
282 These data thus uniquely position methionine as an anabolic cue.

283

284 **Gcn4p regulates only the metabolic response due to methionine**

285 We next asked what the contribution of Gcn4p was towards this methionine mediated
286 metabolic rewiring, at the level of transcription. We first examined global trends of gene
287 expression (similar to those in Figure 2A) in the absence of Gcn4p, compared to WT cells.

288 For this, a relative comparison of transcriptomes of *gcn4Δ* cells grown in RM, MM,
289 MM+Met and MM+nonSAAs to wild-type cells in MM was carried out. To our surprise, the
290 global gene expression trends in the Met set even more strongly resembled the RM set than
291 WT cells (in methionine, from Figure 2A) (Figure 4A). The transcriptional response in all
292 other conditions was almost unaffected (Figure 4A). This unexpectedly suggested that in the
293 absence of *GCN4*, methionine invokes an even stronger transcriptional response, with global
294 trends seemingly resembling a strong "growth state" (Figure 4A). We closely compared
295 transcriptomes of WT cells with *gcn4Δ* cells, under the same combination of conditions used
296 earlier, and analyzed our data with the same stringent filters used in the previous section. The
297 overall changes in transcriptomes of WT vs *gcn4Δ* cells are shown (Figure 4B, Figure S6,
298 Supplementary file E1). In all other conditions except methionine, WT and *gcn4Δ* cells
299 showed similar gene expression profiles (Figure 4B), supporting a unique role for Gcn4p in
300 the Met set. To dissect the role of Gcn4p in the methionine response, we compared relative
301 transcript amounts, for the transcripts induced by methionine, in cells lacking Gcn4p
302 compared to MM. When grouped using GO, we found that a very large number of genes
303 (~200) induced in the presence of methionine, grouped into the general groups of
304 "ribosome/translation", and "nucleotide synthesis" (Figure 4C, Supplementary file E2).
305 Again, this representation was even more striking than that seen in WT cells (Figure 2C),
306 suggesting a strong "growth signature" in the presence of methionine even in cells lacking
307 Gcn4p.

308 Note that (as shown earlier in Figure 1F) Gcn4p was essential for the growth
309 induction due to methionine. These data therefore paradoxically suggested that while the
310 overall "growth signature" response due to methionine was being further amplified in the
311 absence of Gcn4p, only a small subset of Gcn4p regulated genes were pivotal for the
312 metabolic outcome. We therefore more carefully analyzed the classes of transcripts induced

Figure 4

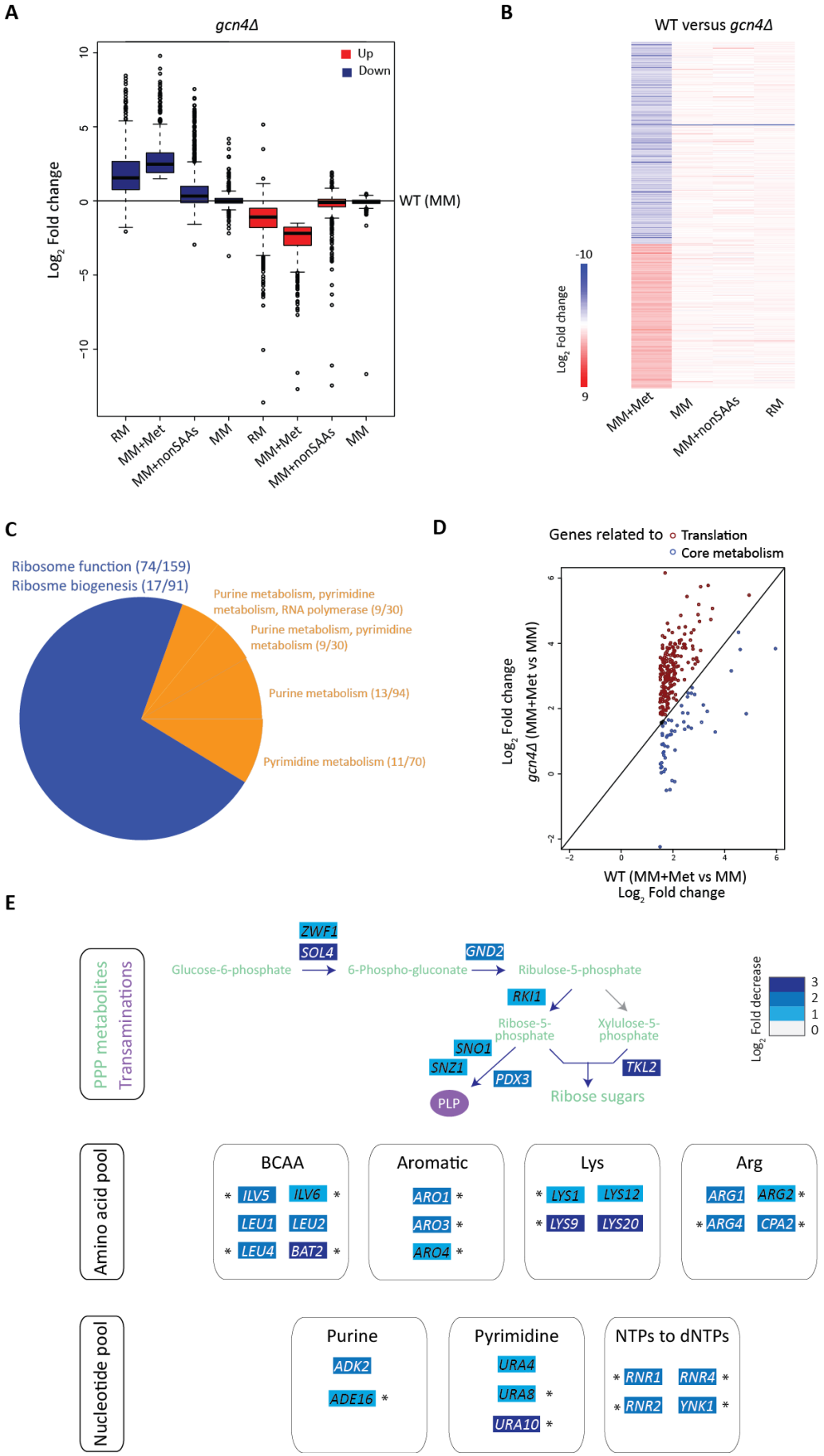
A
gcn4Δ
Up
Down
Log2 Fold change
WT (MM)
RM
MM+Met
MM+nonSAAs
MM
B
WT versus gcn4Δ
Log2 Fold change
-10
9
MM+Met
MM
MM+nonSAAs
RM
C
Ribosome function (74/159)
Ribosme biogenesis (17/91)
Purine metabolism, pyrimidine metabolism, RNA polymerase (9/30)
Purine metabolism, pyrimidine metabolism (9/30)
Purine metabolism (13/94)
Pyrimidine metabolism (11/70)
D
Genes related to
Translation
Core metabolism
Log2 Fold change gcn4Δ (MM+Met vs MM)
WT (MM+Met vs MM) Log2 Fold change
E
PPP metabolites
Transaminations
Glucose-6-phosphate
ZWF1
SOL4
6-Phospho-gluconate
GND2
Ribulose-5-phosphate
RKI1
Ribose-5-phosphate
Xylulose-5-phosphate
SNO1
SNZ1
PDX3
PLP
TKL2
Ribose sugars
Log2 Fold decrease
3
2
1
0
Amino acid pool
BCAA
ILV5
ILV6
LEU1
LEU2
LEU4
BAT2
Aromatic
ARO1
ARO3
ARO4
Lys
LYS1
LYS12
LYS9
LYS20
Arg
ARG1
ARG2
ARG4
CPA2
Nucleotide pool
Purine
ADK2
ADE16
Pyrimidine
URA4
URA8
URA10
NTPs to dNTPs
RNR1
RNR4
RNR2
YNK1

Figure 4: Gcn4p uniquely regulates only the metabolic response due to methionine.

A) Trends of gene expression in RM and methionine supplemented MM in *gcn4Δ* cells. Gene expression levels of transcripts in *gcn4Δ* cells grown in RM or shifted to MM or MM plus methionine or MM plus nonSAAs were compared to WT MM set.

B) Global transcriptional response in the absence of *GCN4*. The heat map shows differentially expressed genes ($\log_2$ 1.5-fold change; $p < 10^{-4}$) between WT and *gcn4Δ* cells in the respective growth conditions.

C) GO analysis of the methionine-responsive genes in *gcn4Δ* cells. A pie chart showing the processes grouped by GO analysis for the up-regulated transcripts between MM plus methionine and MM set in *gcn4Δ* background. Numbers in the bracket indicate the number of genes from the query set/ total number of genes in the reference set for the given GO category.

D) Contribution of *GCN4* to the methionine-response. The expression level of methionine-responsive transcripts in WT set (MM plus methionine versus MM) was compared in the *gcn4Δ* background. Amino acid biosynthesis related genes are marked with blue circles and ribosome biogenesis and function related genes are marked with red circle.

E) Regrouping of the *GCN4*-dependent genes onto metabolic nodes. The schematic shows the *GCN4*-dependent genes (comparison of MM plus methionine set between WT and *gcn4Δ*) in the PPP, amino acid and nucleotide biosynthesis pathways, along with fold-changes in gene expression. The arrows marked blue in the PPP pathway are the steps down-regulated in *gcn4Δ* cells. Key rate-limiting steps in the pathway are marked by asterisk.

313 in WT and *gcn4Δ* cells by methionine (+met), and separated our functional groupings (based
314 on GO) into two broad bins. One bin represented all genes related to ribosome function and
315 translation (as seen in Figure 2C), while the other bin separated out the core metabolic genes
316 (similar to those in Figures 2 and 3) (Figure 4D). Strikingly, transcripts of every gene that
317 mapped to ribosome/translation function (from Figure 2C) was higher in *gcn4Δ* cells
318 compared to WT cells in the presence of methionine (Figure 4D). Contrastingly, every gene
319 related to amino acid biosynthesis (and related metabolism) was significantly lower in the
320 *gcn4Δ* cells (Figure 4D). Thus, this organization revealed that in the presence of methionine,
321 while the induction of the translation machinery, and many "nucleotide synthesis" genes was
322 not Gcn4p dependent, the entire core anabolic rewiring hinged upon Gcn4p.

323 Therefore, we further examined the methionine and Gcn4p dependent transcription of
324 genes that functionally regulated the PPP-GDH-PLP node, or specific steps in amino acid
325 biosynthesis (Figure 4E). Strikingly, the genes from the PPP, and transamination reactions
326 were strongly downregulated in *gcn4Δ* cells compared to WT cells in methionine (Figure 4E).
327 However, the transcript of the Gdh1 enzyme (required for glutamate synthesis) was
328 methionine, but not Gcn4p dependent (Figure 4E). Next, the transcripts of genes encoding
329 key, rate-limiting steps in multiple branched-chain or aromatic amino acid, and lysine and
330 arginine biosynthesis were also methionine and Gcn4p dependent (Figure 4). Finally, while
331 most nucleotide biosynthesis genes were not Gcn4p dependent, the entire RNR complex
332 (critical for the NTP to dNTP conversion, required for DNA synthesis) was strongly
333 methionine and Gcn4p dependent (Figure 4E). Collectively, these data suggest that the core
334 anabolic program induced by methionine is Gcn4p dependent.

335

336 **Methionine stimulates key transamination and reductive biosynthetic processes.**

337 We next directly examined the extent of (i) methionine controlling this anabolic
338 rewiring, through the PPP-GDH-PLP node feeding subsequent anabolic reactions; and (ii),
339 the extent of Gcn4p dependence for these steps. We first tested these possibilities at the
340 biochemical level, comparing the actual enzyme amounts of three key targets that represent
341 the coupling of the PPP with other processes. These are Snz1p, Gnd2p and Gdh1p. Snz1p is
342 required for pyridoxal phosphate (PLP) biosynthesis (Dong *et al*, 2004), which is essential for
343 all transamination reactions (Nelson, DL; Cox, 2017). As illustrated earlier in Figure 2D, PLP
344 biosynthesis itself requires the PPP intermediate erythrose-4-phosphate as a substrate. Gnd2p
345 is the key NADPH generating enzyme in the oxidative branch of the PPP. Gdh1p consumes
346 NADPH and makes glutamate from 2-ketoglutarate. We measured amounts of these three
347 proteins from WT and *gcn4Δ* cells growing in MM, and MM+methionine (Figure 5A).
348 Notably, Snz1p and Gnd2p showed a strong induction that was both methionine dependent,
349 and dependent on Gcn4p (Figure 5A, Figure S7). Gdh1p was strongly dependent upon
350 methionine, but was less dependent on Gcn4p (Figure 5A). We next measured *in vitro* Gdh1p
351 activity (NADPH-GDH activity) in lysates from cells growing in MM or with methionine,
352 and found that overall Gdh1p activity was higher in cells growing with methionine (Figure
353 5B). However, as seen in the Western blot analysis (Figure 5A), the *in vitro* Gdh1p activity
354 was not dependent on Gcn4p (not shown). All these data strongly support the observation that
355 methionine drives these key, coupled steps in biosynthesis, and that they are largely mediated
356 by Gcn4p. Finally, an expected crude readout of this biochemical coupling should be changes
357 in steady-state nucleotide amounts, with a Gcn4p dependence in methionine replete
358 conditions. Comparing relative amounts of nucleotides in wild-type and *gcn4Δ* cells, we
359 noted a decrease in the nucleotide amounts in *gcn4Δ* cells in the presence of methionine
360 (Figure 5C). Collectively, these direct biochemical read-outs support our proposed paradigm

Figure 5

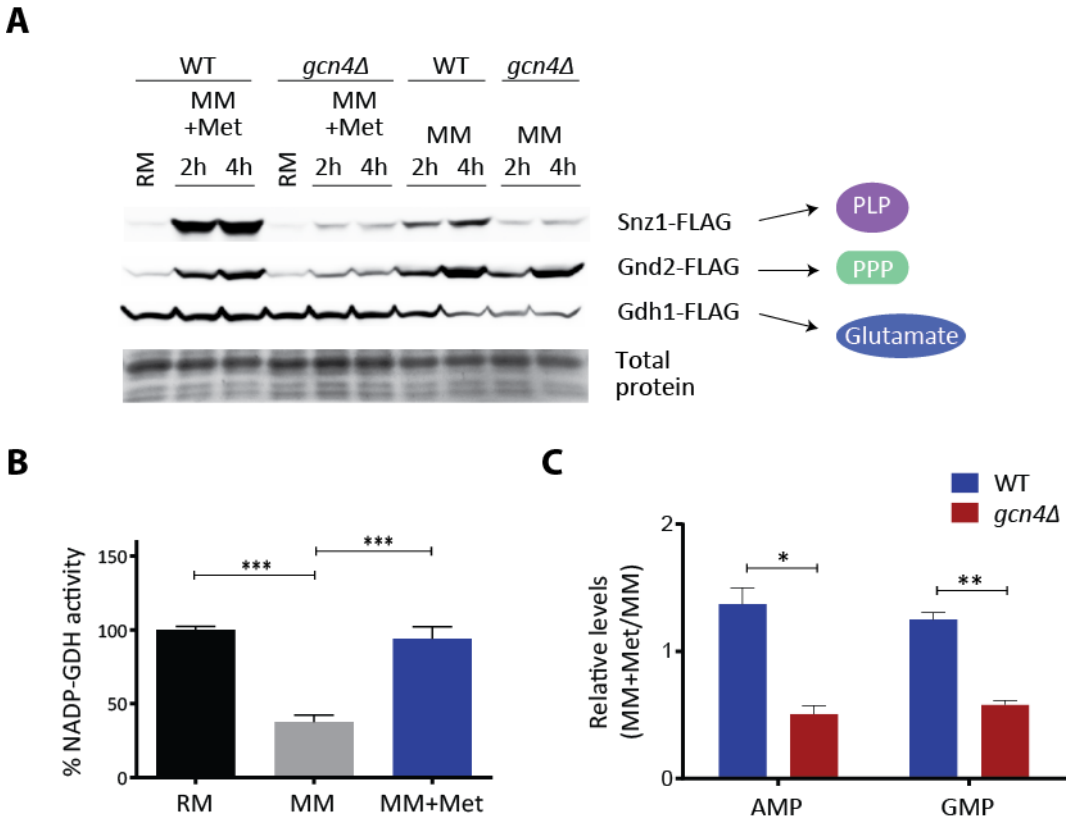

Figure 5: Methionine stimulates key transamination and reductive biosynthetic processes.

A) Snz1p, Gnd2p and Gdh1p amounts in WT or *gcn4Δ* cells. WT and *gcn4Δ* cells expressing FLAG-tagged Snz1p or Gnd2p or Gdh1p were shifted from RM to MM or MM plus methionine and amounts of these proteins were detected by Western blotting. A representative blot is shown in each case.

B) NADP-dependent glutamate dehydrogenase activity and methionine availability. Crude extracts of WT cells grown in RM and shifted to MM or MM plus methionine were analysed for intracellular biosynthetic NADP-glutamate dehydrogenase activity.

C) Relative nucleotide amounts in the presence of methionine in WT or *gcn4Δ* cells. WT and *gcn4Δ* cells grown in RM were shifted to MM (4h) with and without methionine, and the relative amounts of AMP and GMP from metabolite extracts of the respective samples were measured by LC-MS/MS.

In all panels data indicate mean±SD values. $^{*}p < 0.05$, $^{**}p < 0.01$, $^{***}p < 0.001$.

361 of a coupled induction of the PPP, and key transamination reactions by methionine, leading to
362 increased amino acid and nucleotide synthesis.

363

364 **Methionine induces *de novo* biosynthesis of key amino acids.**

365 Substantiating these findings using steady-state metabolite measurements alone is
366 insufficient (and often misleading), since any steady-state metabolite measurement (as in
367 Figure 5C) cannot directly distinguish synthesis from consumption. Therefore, to directly
368 address this possible hierarchical anabolic program, we resorted to a stable-isotope pulse
369 labelling and LC-MS/MS based approach to directly measure the new synthesis of amino
370 acids. To WT or *gcn4Δ* cells in the respective medium with or without methionine, we pulsed
371 ^{15}N-labelled ammonium sulfate, and measured the ^{15}N incorporation into amino acids (Figure
372 6A, Table S2), before an effective steady-state of labelled amino acid synthesis and
373 consumption was reached. This permits the detection of newly synthesized amino acids,
374 which will incorporate the ^{15}N label. We observed that biosynthesis of all the aromatic amino
375 acids, lysine, histidine, proline, arginine and asparagine is strongly dependent on methionine
376 presence (Figure 6B). For technical reasons we could not measure label-incorporation into
377 branched-chain amino acids. Notably, the label immediately (~20 min) percolated in
378 asparagine and aromatic amino acid biosynthesis, and showed a very strong methionine
379 dependence (Figure 6B). Asparagine, proline and phenylalanine biosynthesis were
380 methionine dependent even in *gcn4Δ* cells, pointing towards possible *GCN4*-independent
381 influences of methionine. For all the other amino acids measured, the biosynthesis was both
382 methionine as well as *GCN4*-dependent (Figure 6B). These data directly indicate that
383 methionine availability controls the key nodes around PPP-PLP-GDH axis, thereby
384 generating the amino acid pool required for proliferation.

Figure 6

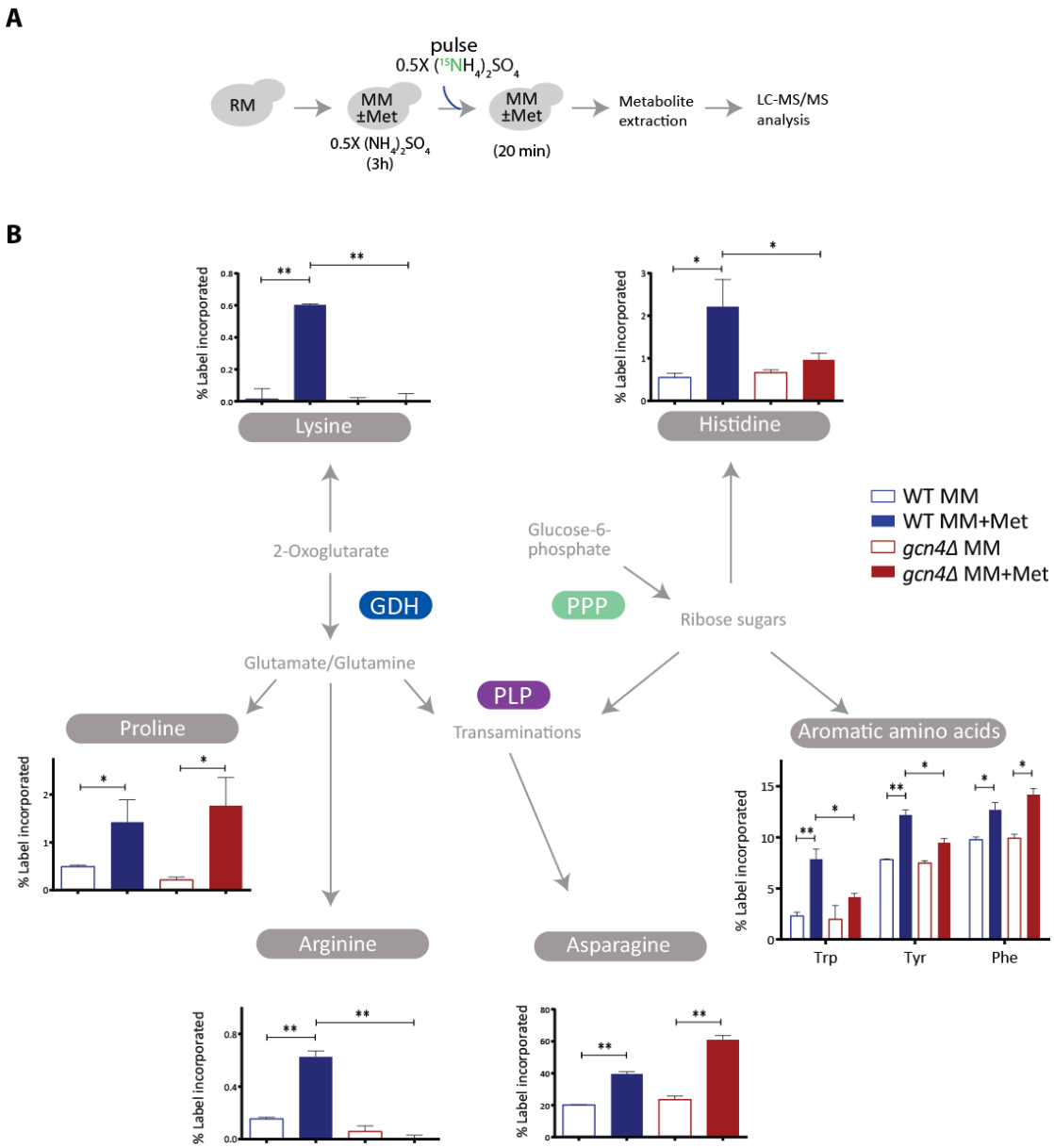

Figure 6: Methionine induces *de novo* amino acid biosynthesis

A) A schematic showing the experimental design of ^{15}N pulse-labelling experiment. Cells were shifted to MM with and without methionine, maintained for 3h. ^{15}N-ammonium sulfate was then pulsed into the medium, and the indicated, labelled metabolites were measured. The data shown is after 20 min of pulsing. Also see Table S2.

B) Methionine increases nitrogen assimilation in amino acids. Label incorporation in newly synthesized amino acids in WT and *gcn4Δ* cells was measured, as shown in the panel A. For all the labelled moieties, fractional abundance of the label was calculated. Also see Table S2.

In all panels data indicate mean±SD values. $^{*}p < 0.05$, $^{**}p < 0.01$.

385

386 **Methionine increases nucleotide biosynthesis in a Gcn4p dependent manner.**

387 Given that the PPP and amino acid biosynthesis are directly regulated by methionine
388 and Gcn4p, and the PPP and amino acids together couple to nucleotide synthesis, we
389 predicted that collectively, perturbing this node should have a severe consequence on
390 nucleotide biosynthesis, regardless of nucleotide biosynthesis genes themselves being directly
391 regulated by Gcn4p. In principle, this also will reflect flux through the coupled steps of the
392 PPP, glutamate/glutamine synthesis, and the use of intermediates from amino acid
393 biosynthetic pathways for carbon and nitrogen assimilation into nucleotides (Figure 7A). The
394 carbon skeleton of nucleotides comes from the PPP, the nitrogen base is directly derived from
395 glutamine/glutamate and aspartate, and glutamate synthesis is itself coupled to NADPH (from
396 the PPP) (Figure 7A). Nucleotide biosynthesis is also coupled to histidine and tryptophan
397 synthesis. We therefore adopted a direct estimation of methionine and Gcn4p dependent
398 increases in nucleotide synthesis (similar to the approach in Figure 6), predicting an increase
399 in *de novo* nucleotide synthesis due to methionine, coming from the earlier amino acid
400 precursors. To this end, using a stable-isotope based nitrogen or carbon pulse labelling
401 approach, coupled to targeted LC-MS/MS based measurement of nucleotides, we separately
402 measured the incorporation of the nitrogen and carbon label into nucleotides, as illustrated in
403 Figure 7B and 7C. We observed a dramatic increase in ^{15}N-labelled nucleotides upon the
404 addition of methionine, in ~1 hour (Figure 7B, Table S2). Furthermore, this methionine-
405 mediated incorporation of ^{15}N-label in nucleotides was entirely Gcn4p dependent (Figure 7B
406 and Figure S8).

407 Monitoring carbon flux is extremely challenging in a non-fermentable carbon source
408 like lactate (as compared to glucose), given the difficulties of following the labelled carbon

Figure 7

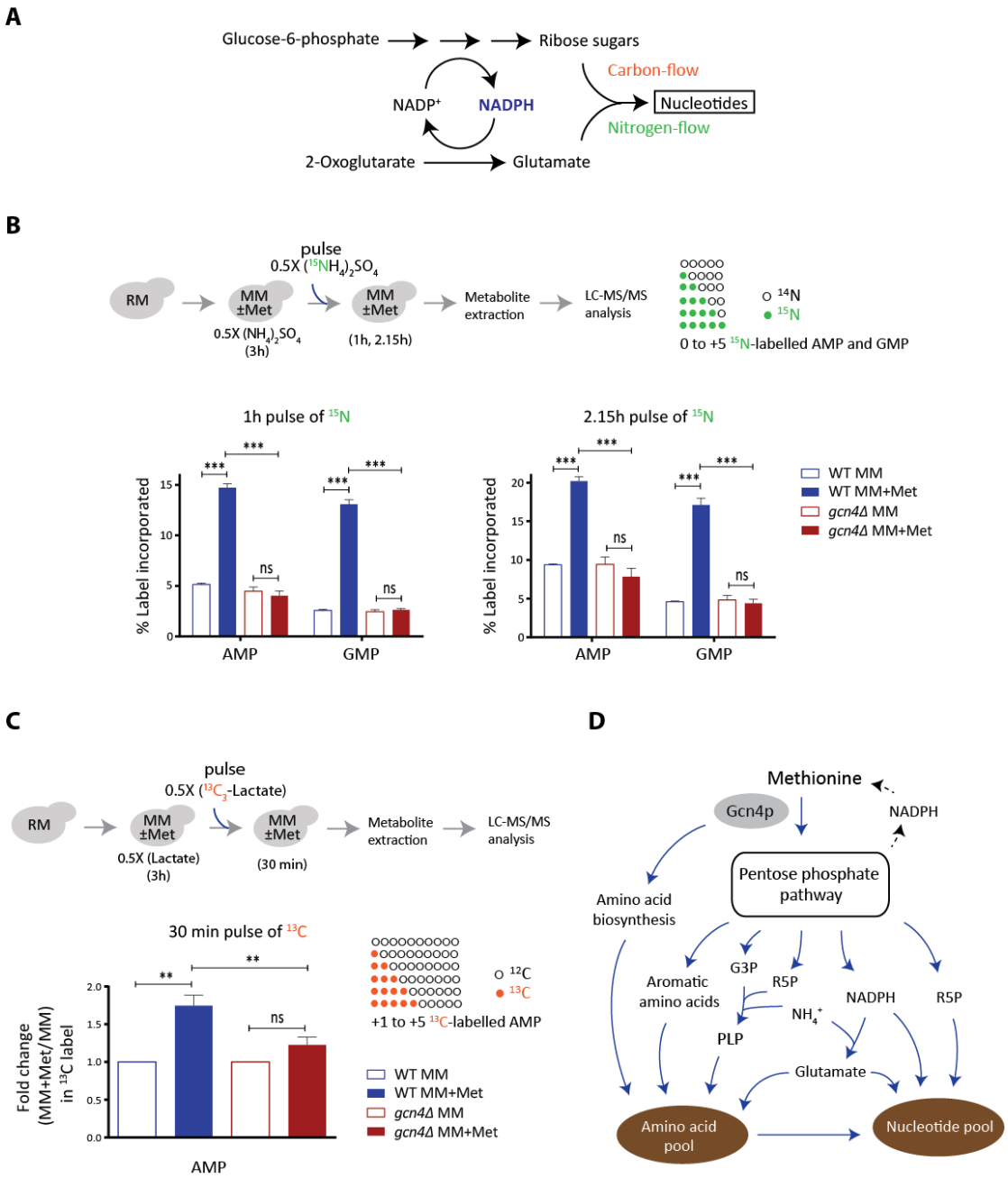

Figure 7: Methionine increases nucleotide biosynthesis in a Gcn4p dependent manner.

A) A schematic showing carbon and nitrogen inputs in nucleotide biosynthesis, and their coupling to the PPP/NADPH metabolism.

B) Methionine increases nitrogen assimilation in nucleotides. The WT and *gcn4Δ* cells treated and pulse-labelled with ^{15}N ammonium sulfate as illustrated in the top panel. For all the labelled moieties, fractional increase of the incorporated label was calculated, to measure newly synthesized AMP and GMP. (also see Figure S8 for CMP and UMP).

C) Methionine enhances carbon flux into AMP biosynthesis. An experimental set-up similar to the Panel B was employed, using ^{13}C-lactate for carbon labelling. Label incorporation into nucleotides (from +1 to +5) was accounted for calculations. (note: GMP could not be

estimated because of MS/MS signal interference from unknown compounds in the metabolite extract).

E) A model illustrating how methionine triggers cell proliferation. Methionine activates the *GCN4*-mediated ISR, promoting the synthesis of PPP metabolites, PLP, NADPH and glutamate (up-regulated genes in the pathways are shown in blue), which directly feed into nitrogen metabolism. As a result, methionine activates biosynthesis of amino acids and nucleotides, allowing the cells to grow in amino acid limiting medium.

In all panels data indicate mean±SD. ns: non-significant difference, $^{**}p < 0.01$, $^{***}p < 0.001$.

409 molecules. Despite that, like the ^{15}N-labeling experiments described above, a similar
410 experimental design of 0.5X-label spiking was adopted to measure the ^{13}C-label
411 incorporation into AMP (Figure 7C, Table S2). We observed a significant increase in ^{13}C-
412 labelled AMP upon the addition of methionine, and this methionine dependent incorporation
413 of ^{13}C-label in AMP was not observed in cells lacking Gcn4p (Figure 7C). Collectively, these
414 data show a methionine and Gcn4p dependent increase in *de novo* synthesis of nucleotides,
415 coupling carbon and nitrogen flux that is dependent on the PPP, and glutamate synthesis.
416 Note that the kinetics of incorporation of label are entirely in line with the predicted
417 hierarchy. Increased amino acid labels (from Figure 6) were seein in ~20 min post labelled
418 ammonium sulfate addition, while the nucleotide label increase occurs in ~1 hr, subsequent to
419 the observed amino acid label increase. Thus, we directly demonstrate first the synthesis of
420 new amino acids, and the subsequent synthesis of nucleotides, in a methionine and Gcn4p
421 dependent manner.

423 **Discussion**

424 In this study, we show how methionine drives cellular proliferation by rewiring cells
425 to an anabolic state, even under otherwise amino acid limited, challenging conditions. We
426 uncover a regulated, hierarchical activation of metabolic processes by methionine, which
427 leads to overall anabolism. We also present a mechanism of how methionine mediates this
428 anabolic program.

429 Starting with a framework of existing models for responses to amino acid limitation
430 (Figure 1), we systematically build the underlying metabolic foundations of a methionine
431 mediated anabolic state switch. Methionine mediates a global transcriptional remodelling in
432 cells, thereby controlling the anabolic program (Figures 2, 4). Understanding the core
433 metabolic logic within the transcriptional response to methionine necissitated a biochemical
434 first principles based approach, emphasizing control points at rate or resource limiting
435 biochemical steps. The organizational metabolic logic that emerged was striking (Figure 2, 3
436 and 4). First, methionine positively regulates the PPP (Figure 2). The PPP provides the
437 pentose sugar backbones for nucleotides, along with reducing equivalents (NADPH),
438 allowing reductive biosynthesis for a variety of anabolic molecules (Nelson, DL; Cox, 2017).
439 For amino acid and nucleotide synthesis, pyridoxal phosphate, which controls all
440 transamination reactions, is also essential (Eliot & Kirsch, 2004), and methionine directly
441 induced this node as well (Figure 2). Collectively, methionine strongly induced the PPP-
442 GDH-PLP node (Figure 2). These three nodes can feed all the subsequent metabolic steps
443 induced by methionine. Furthermore, in these subsequent anabolic nodes (the synthesis of
444 amino acids and nucleotides), methionine only induces the expression of genes that control
445 rate limiting or final steps (Figure 3). These biosynthetic nodes include those that synthesize
446 what are considered the "costliest" amino acids, namely the aromatic amino acids and the
447 branch chain amino acids (Figure 3). Notably, essentially every one of these (methionine

448 regulated) steps use cofactors or intermediates from the the PPP-GDH-PLP node (Figure 2
449 and 3). Thus, it appears that methionine sets up this striking metabolic hierarchy, as
450 illustrated in a schematic in Figure 3C and 7D.

451 Interestingly, the methionine dependent growth and increased activity in most of these
452 metabolic nodes, and thus the overall anabolic program, depends upon Gcn4p (Figure 1,
453 Figure 4). Gcn4p is best understood as a regulator of amino acid biosynthesis during
454 starvation (Natarajan *et al*, 2001). Many of the *GCN4* targets picked up in our study compare
455 well with the landmark study of *GCN4* targets (Natarajan *et al*, 2001) (see Figure S9 and
456 Table S3). However, this role of Gcn4p in the presence of methionine in synchronously
457 controlling these key hubs of the PPP, transamination reaction, glutamate biosynthesis,
458 coupled with rate-regulating steps in costly amino acid and nucleotide biosynthesis has not
459 been previously appreciated. Furthermore, in this context Gcn4p enables anabolism and
460 increased proliferation, and not just survival during starvation. Also interestingly, Gcn4p
461 appears to regulate only the core metabolic program induced by methionine, and not the
462 induction in the synthesis of the translation machinery (as seen in Figure 4). This induction of
463 translation due to methionine might be through other mechanisms, including activation of the
464 TOR pathway (Sutter *et al*, 2013; Laxman *et al*, 2014b). Finally, a combination of rigorous
465 biochemical, and metabolic flux based analysis using stable-isotopes directly demonstrate
466 this hierarchical coupling of the PPP, NADPH utilization and transamination reactions (in
467 both nitrogen assimilation and carbon assimilation) first towards the increased synthesis of
468 aromatic and branch-chain amino acids, and next towards nucleotides, in a methionine and
469 Gcn4p dependent manner (Figures 6, 7). Collectively, our data permits the construction of an
470 overall pyrimidical hierarchy of metabolic events, mediated by methionine, to set up an
471 anabolic program (model in Figure 3C). This reveals general organizational principles by
472 which cells can specifically rewire metabolism. These data also show how methionine can

473 co-opt Gcn4p, thought to be primarily important for survival, to achieve an anabolic,
474 proliferative state.

475 The central role of the PPP in anabolism is text-book knowledge (Nelson, DL; Cox,
476 2017). Yet, a better appreciation of the importance of the PPP in mediating an anabolic
477 rewiring is now emerging due to the association of the PPP to cancer metabolism (Patra &
478 Hay, 2014; Cairns *et al*, 2011). Many anabolic transformations require contributions from the
479 PPP, however, the metabolic cues regulating the PPP (and coupling to other processes) are
480 not often obvious. Additionally, these studies ignore or underplay coincident but necessary
481 metabolic events for proliferation. Our study directly addresses how methionine (likely
482 through its downstream metabolite SAM), acts as an anabolic signal for cells, through setting
483 up of the metabolic hierarchy explained earlier, with the co-incident PLP and glutamine
484 nodes being critically important. This striking role of methionine as an anabolic cue seems
485 analogous to another central metabolite, acetyl-CoA, which is better known to determine
486 cellular decisions towards growth (Comerford *et al*, 2014; Shi & Tu, 2013; Pedro & Madeo,
487 2015; Mariño *et al*, 2014; Cai *et al*, 2011). Interesting correlations can be made from our
488 observations to known roles of methionine in cancer cell metabolism, and metazoan growth.
489 The earliest observations of methionine as important for proliferation in some cancers dates
490 back to the 1950s (Cavuoto & Fenech, 2012; Sugimura *et al*, 1959; Breillout *et al*, 1990), and
491 several types of cancer cells are addicted to methionine (Halpern *et al*, 1974; Stern &
492 Hoffman, 1986; Guo *et al*, 1993; Lu & Epner, 2000; Poirson-Bichat *et al*, 2000; Kokkinakis
493 *et al*, 2001; Cellarier *et al*, 2003; Clarke *et al*, 2016; Cavuoto & Fenech, 2012). Other, distinct
494 studies show that *Drosophila* fed on methionine rich diets exhibit rapid growth, high
495 fecundity, and shorter lifespans (Troen *et al*, 2007; Lee *et al*, 2016, 2014), all hallmarks of
496 what a "proliferative" metabolite will do. Studies from yeast show how methionine inhibits
497 autophagy, or regulates the TORC1 to boost growth (Sutter *et al*, 2013; Laxman *et al*, 2013,

498 2014a). One of the earliest known cell cycle entry check-points found in yeast links to
499 methionine (Unger & Hartwell, 1976). Upon sulfate (and thereby methionine) starvation,
500 yeast cells arrest their growth to promote survivability (Boer *et al*, 2008), and transform their
501 proteome to preferentially express proteins containing fewer cysteine/methionine residues to
502 save sulfur (Lagniel *et al*, 2002). There are other, less appreciated observations connecting
503 methionine metabolism and the PPP. Yeast cells lacking *ZWF1* (glucose-6-phosphate
504 dehydrogenase, the first enzyme in the PPP) exhibit methionine auxotrophy (Thomas *et al*,
505 1991), and methionine supplementation also increases the oxidative stress tolerance of *zwf1Δ*
506 (Campbell *et al*, 2016). Despite these studies highlighting a critical role of methionine, such a
507 hierarchical logic explaining the organizational principles of the anabolic program mediated
508 by methionine, and the mechanisms by which this is mediated, has thus far been elusive. Our
509 study provides this.

510 Our use of a "less-preferred" carbon source, lactate, has helped reveal regulatory
511 phenomena otherwise hidden in glucose and amino acid rich laboratory conditions, where a
512 surfeit of costly metabolic resources (for example, unlimited PPP intermediates) are present.
513 Interestingly, several recent reports emphasize the importance of lactate as a carbon source in
514 rapidly proliferating cells (Kennedy *et al*, 2013; Faubert *et al*, 2017; Hu *et al*, 2017), and our
515 observations might inform how proliferation is achieved in these conditions. Furthermore, the
516 so called integrated stress response (ISR), and the Gcn4p ortholog in mammals, Atf4, play
517 important roles in cancer cell proliferation (Bi *et al*, 2005; Palam *et al*, 2015; Ye *et al*, 2010),
518 where many cancers continue to grow in apparently poor nutrient environments. Our study
519 suggests how, in methionine rich (but otherwise amino acid limiting) conditions, Gcn4/Atf4
520 might function to promote growth, and not just help cells recover from nutrient stress. A
521 separate, emerging question will be to understand how Gcn4p is itself regulated under these
522 otherwise amino acid limited conditions, by methionine. Note that our studies would not have

been possible without using prototrophic ("wild type") yeast strains to study responses to amino acids. Typically, studies utilize laboratory strains derived from an auxotrophic backgrounds (eg. S288C/BY4741), which require supplemented uracil, histidine, leucine and methionine for survival (Sherman, 1991; Pronk, 2002; Corbacho *et al*, 2011; Brachmann *et al*, 1998; Gerashchenko & Gladyshev, 2014; Alam *et al*, 2016), and where therfore overall amino acid homeostasis is severely altered. This precludes systematic experiments with amino acid limitation, such as those in this study.

We close by suggesting a possible metabolic cost based hypothesis for what might make methionine a strong growth cue. The *de novo* synthesis of methionine and its immediate metabolites (notably SAM) is exceptionally costly in terms of NADPH molecules invested (Thomas *et al*, 1997; Kaleta & Schäuble, 2013; Mampel *et al*, 2005; Sutter *et al*, 2013). Cells require at least 6 molecules of NADPH to reduce sulfur and synthesize a single molecule of methionine. Since biology has tied multiple anabolic processes to reductive biosynthesis (dependent on NADPH from the PPP), the availability of methionine might be an ancient signal to represent a metabolic state where reductive equivalents are sufficiently available for all other reductive biosynthetic processes as a whole.

540 **Materials and Methods:**

541 **Yeast strains and growth media**

542 The prototrophic CEN.PK strain (referred to as wild type, WT) was used in all experiments
543 (van Dijken JP *et al*, 2000). Strains with gene deletions or chromosomally tagged proteins (at
544 the C-terminus) were generated as described. Strains used in this study are listed in Table S1.

545 The growth media used in this study are RM (1% yeast extract, 2% peptone and 2% lactate)
546 and MM (0.17% yeast nitrogen base without amino acids, 0.5% ammonium sulfate and 2%
547 lactate). All amino acids were supplemented at 2 mM. NonSAAs refers to the mixture of all
548 standard amino acids (2 mM each) except methionine, cysteine and tyrosine.

549 The indicated strains were grown in RM with repeated dilutions (~36 hours), and the culture
550 in the log phase (absorbance at 600 nm of ~1.2) was subsequently switched to MM, with or
551 without addition of the indicated amino acids. For growth curves, the RM acclimatized
552 cultures were used and diluted in a fresh medium with the starting absorbance of ~0.2 and the
553 growth was monitored at the indicated time intervals.

554 **Polysome analysis**

555 The cells (50 OD) were treated with cycloheximide (100 µg/ml) for 15 minutes before
556 harvesting in ice-filled, cold centrifuge bottles. The pellet obtained after centrifugation
557 (8000g, 5 min, 4°C) was once washed, and then re-suspended in 0.5 ml lysis buffer (10 mM
558 Tris-HCl pH 7, 0.1 M NaCl, 30 mM $MgCl_2$, 1U/µl Ribolock RNase inhibitor and 80 µg/ml
559 cycloheximide) with chilled, baked acid-washed glass beads. After bead-beating, 0.5 ml lysis
560 buffer was added and the crude extract obtained was centrifuged (18407g, 10 min, 4°C) and
561 the supernatant (200 µl) containing polysomes is fractionated on a sucrose gradient (7%-47%
562 sucrose; containing 20 mM Tris-HCl pH 7, 140 mM KCl, 5 mM $MgCl_2$, 1 mM DTT and 50

563 μg/ml cycloheximide) by ultra-centrifugation (35000 rpm, 3 h, 4°C). The polysome profile
564 was obtained on an ISCO fractionator, wherein the absorbance at 254 nm was traced. For
565 polysome: monosome ratio calculation, area under the curve was quantified using ImageJ
566 software (*Rasband, ImageJ*, U. S. National Institutes of Health, Bethesda, Maryland, USA,
567 http://imagej.nih.gov/ij/, 1997-2016).

568 **Western blot analysis**

569 Approximately ten OD_{600} cells were collected from respective cultures, pelleted and flash-
570 frozen in liquid nitrogen until further use. The cells were re-suspended in 400 μl of 10%
571 trichloroacetic acid and lysed by bead-beating three times: 30 sec of beating and then 1 min
572 of cooling on ice. The precipitates were collected by centrifugation, re-suspended in 400 μl of
573 SDS-glycerol buffer (7.3% SDS, 29.1% glycerol and 83.3 mM Tris base) and heated at
574 100°C for 10 min. The supernatant after centrifugation was treated as the crude extract.
575 Protein concentrations from extracts were estimated using bicinchoninic acid assay (Thermo
576 Scientific). Equal amounts of samples were resolved on 4 to 12% Bis-Tris gels (Invitrogen).
577 Coomassie blue–stained gels were used as loading controls. Western blots were developed
578 using the antibodies against the respective tags. We used the following primary antibodies:
579 monoclonal FLAG M2 (Sigma), HA (12CA5, Roche), and phosphor-eIF2α Ser51 (9721, Cell
580 Signaling). Horseradish peroxidase–conjugated secondary antibodies (mouse and rabbit)
581 were obtained from Sigma. For Western blotting, standard enhanced chemiluminescence
582 reagents (GE Healthcare) were used. ImageJ was used for quantification.

583 **Immunofluorescence measurements**

584 Yeast cells were fixed with 3.7% formaldehyde, washed and resuspended in spheroplasting
585 buffer (40 mM potassium phosphate buffer, pH 6.5; 0.5 mM $MgCl_2$; 1.2 M sorbitol).
586 Spheroplasts were prepared by zymolyase (MP Biomedicals, 08320921) treatment and spread

587 on a slide pretreated with 50 µl of 1 mg/ml polylysine (Sigma-Aldrich, P6407). Gcn4-HA
588 was stained with the mouse monoclonal anti-HA (12CA5) primary antibody (Roche,
589 11583816001) and Alexa Fluor 488-conjugated Goat anti-Mouse IgG (H+L) secondary
590 antibody (Thermofisher, A32723). DNA was stained with 1µg/ml DAPI for 2 minutes,
591 washed and mounted in Fluoromount-G (Southern Biotech, 0100-01). The cells were imaged
592 using Olympus FV1000 confocal microscope.

593 **RNA-seq analysis:**

594 Total RNA from yeast cells was extracted using hot acid phenol method (Collart & Oliviero,
595 2001). The quality of RNA was checked on Bioanalyzer using an RNA 6000 Nano kit
596 (Agilent) and the libraries were prepared using TruSeq RNA library preparation kit V2
597 (Illumina). The samples were sequenced on Illumina platform HiSeq2500. The raw data is
598 available with NCBI-SRA under the accession number SRP101768. Genome and the
599 annotation files of *S. cerevisiae* S288C strain were downloaded from Saccharomyces
600 Genome Database (SGD; http://www.yeastgenome.org/). 100-mer, single-end reads obtained
601 from RNA sequencing experiments were mapped to the S288C genome using Burrows
602 Wheeler Aligner (BWA) (Li & Durbin, 2009). Mapped reads with the mapping quality of ≥
603 20 were used for the further analysis. The number of reads mapped to each gene was
604 calculated and the read count matrix was generated. The read count matrix was fed into
605 EdgeR, a Bioconductor package used for analyzing differential gene expression (Robinson *et*
606 *al*, 2010). Genes which are differentially expressed by at least 3-fold with the p-value of
607 <0.0001 were considered for further analysis. Normalized gene expression was calculated by
608 dividing the number of reads by the gene length and the total number of reads for those
609 samples, then dividing each of these values with the mode of its distribution (Srinivasan *et al*,
610 2013). Absolute expression levels of the genes between the replicates are well correlated
611 with the Pearson correlation coefficient (R) values more than 0.99 (see Figure S2). Mapping

612 of genes to the related pathways and gene ontology analysis were carried out using public
613 databases such as Yeastcyc (Caspi *et al*, 2014), GeneCodis (Tabas-Madrid *et al*, 2012;
614 Nogales-Cadenas *et al*, 2009; Carmona-Saez *et al*, 2007) and SGD (Dwight *et al*, 2002).

615 **Metabolite extractions and measurements by LC-MS/MS**

616 Cells were grown in RM for ~36 hours and transferred to MM with and without methionine
617 for the indicated time. After incubation, cells were rapidly harvested and metabolite extracted
618 as described earlier (Tu *et al*, 2007). Metabolites were measured using LC-MS/MS method
619 as described earlier (Laxman *et al*, 2014a). Standards were used for developing multiple
620 reaction monitoring (MRM) methods on Thermo Scientific TSQ Vantage triple stage
621 quadrupole mass spectrometer or Sciex QTRAP 6500. For positive polarity mode,
622 metabolites were separated using a Synergi 4µ Fusion-RP 80A column (150 × 4.6 mm,
623 Phenomenex) on Agilent's 1290 infinity series UHPLC system coupled to mass spectrometer.
624 Buffers used for separation were: buffer A: 99.9% H_2O/0.1% formic acid and buffer B:
625 99.9% methanol/0.1% formic acid (Flow rate, 0.4 ml/min; T = 0 min, 0% B; T = 3 min, 5%
626 B; T = 10 min, 60% B; T = 10.1 min, 80% B; T = 12 min, 80% B; T = 14 min, 5% B; T = 15
627 min, 0% B; T = 20 min, stop). For negative polarity mode, metabolites were separated using
628 a Luna HILIC 200A column (150 × 4.6 mm, Phenomenex). Buffers used for separation were:
629 buffer A: 5 mM ammonium formate in H_2O and buffer B: 100% acetonitrile (flow rate: 0.4
630 ml/min; T = 0 min, 95% B; T = 1 min, 40% B; T = 7 min, 10% B; T = 11 min, 1% B; T = 13
631 min, 95% B; T = 17 min, stop). The area under each peak was calculated using Thermo
632 Xcalibur software (Qual and Quan browsers).

633 **^{15}N- and ^{13}C- based metabolite labelling experiments**

634 For detecting ^{15}N-label incorporation in amino acids and nucleotides, ^{15}N-ammonium sulfate
635 with all nitrogens labelled (Sigma- Aldrich) was used. For ^{13}C-labeling experiment, ^{13}C-

636 lactate with all carbons labelled (Cambridge Isotope Laboratories) was used. In the labelling
637 experiments, 0.5X refers to 0.25% ammonium sulfate or 1% lactate. All the parent/product
638 masses measured are enlisted in Table S2. Amino acid measurements were done in the
639 positive polarity mode. For all the nucleotide measurements, release of the nitrogen base was
640 monitored in positive polarity mode. For the ^{13}C-label experiment, the phosphate release was
641 monitored in negative polarity mode. Under these conditions, the nitrogen base release cannot
642 be monitored here as the nitrogen base itself has carbon skeleton, which will complicate the
643 analysis. The HPLC and MS/MS protocol was similar to those explained above.

644 **GDH assays**

645 Glutamate dehydrogenase activity was measured as described in (Doherty, 1970), with some
646 modifications. Yeast cells were lysed by bead-beating in lysis buffer (100 mM potassium
647 phosphate buffer, pH 7; 5% glycerol; 1 mM PMSF; 0.1% Tween-20; 1 mM EDTA; 1 mM 2-
648 mercaptoethanol). NADP-dependent activity was measured by monitoring oxidation of
649 NADPH (assay buffer: 100 mM Tris-HCl, pH 7.2; 10 mM 2-ketoglutarate, pH adjusted to
650 7.2; 100 mM ammonium chloride; 0.1 mM NADPH) at 340 nm. Protein concentrations from
651 extracts were estimated using bicinchoninic acid assay (Thermo Scientific). One enzyme unit
652 corresponds to the amount of enzyme required to oxidize one μmol of NADPH min^{-1} at room
653 temperature.

654 **Statistical analysis**

655 In most experiments, Student's t-test was applied for calculating the p-values. Wherever
656 necessary, other tests were applied and indicated accordingly.

657

658

Acknowledgements:

We acknowledge Dhananjay Shinde, Padma Ramakrishnan and the NCBS/inStem/C-CAMP Mass spectrometry facility for LC-MS/MS support, Avadheesh Pandit and the NCBS/inStem/C-CAMP next-generation sequencing facility for assistance with library preparation, and Ravi Muddashetty for the polysome fractionator. We thank Utpal Banerjee, Mark Sharpley, Marco Foiani, Christopher Bruhn, Krishnamurthy Natarajan, Arati Ramesh and PJ Bhat for critical comments on this manuscript. This work was supported by a Wellcome Trust-DBT IA intermediate fellowship (IA/I/14/2/501523) and inStem/DBT institutional support to SL. ASW, RG, RS acknowledge bridging fellowships (from inStem), and ASW, RG and RS are supported by DST SERB-national postdoctoral fellowships (PDF/2015/000225, PDF/2016/000416 and PDF/2016/001877 respectively).

670 **References:**

671 Alam MT, Zelezniak A, Mülleder M, Shliaha P, Schwarz R, Capuano F, Vowinckel J,
672 Radmaneshfar E, Krüger A, Calvani E, Michel S, Börno S, Christen S, Patil KR,
673 Timmermann B, Lilley KS & Ralser M (2016) The metabolic background is a global
674 player in Saccharomyces gene expression epistasis. *Nat. Microbiol.* **1:** 15030 Available
675 at: http://www.nature.com/articles/nmicrobiol201530

676 Barton MD, Delneri D, Oliver SG, Rattray M & Bergman CM (2010) Evolutionary Systems
677 Biology of Amino Acid Biosynthetic Cost in Yeast. *PLoS One* **5:** e11935

678 Bi M, Naczki C, Koritzinsky M, Fels D, Blais J, Hu N, Harding H, Novoa I, Varia M,
679 Raleigh J, Scheuner D, Kaufman RJ, Bell J, Ron D, Wouters BG & Koumenis C (2005)
680 ER stress-regulated translation increases tolerance to extreme hypoxia and promotes
681 tumor growth. *EMBO J.* **24:** 3470–81

682 Boer VM, Amini S & Botstein D (2008) Influence of genotype and nutrition on survival and
683 metabolism of starving yeast. *Proc. Natl. Acad. Sci.* **105:** 6930–6935

684 Boer VM, Crutchfield CA, Bradley PH, Botstein D & Rabinowitz JD (2010) Growth-limiting
685 Intracellular Metabolites in Yeast Growing under Diverse Nutrient Limitations. *Mol.*
686 *Biol. Cell* **21:** 198–211

687 Brachmann CB, Davies A, Cost GJ, Caputo E, Li J, Hieter P & Boeke JD (1998) Designer
688 deletion strains derived from Saccharomyces cerevisiae S288C: a useful set of strains
689 and plasmids for PCR-mediated gene disruption and other applications. *Yeast* **14:** 115–
690 32

691 Brauer MJ, Huttenhower C, Airoldi EM, Rosenstein R, Matese JC, Gresham D, Boer VM,
692 Troyanskaya OG & Botstein D (2008) Coordination of Growth Rate, Cell Cycle, Stress
693 Response, and Metabolic Activity in Yeast. *Mol. Biol. Cell* **19:** 352–267

694 Breillout F, Antoine E & Poupon MF (1990) Methionine dependency of malignant tumors: a

695 possible approach for therapy. *J. Natl. Cancer Inst.* **82:** 1628–32
696 Broach JR (2012) Nutritional Control of Growth and Development in Yeast. *Genetics* **192:**
697 73–105 Available at: http://www.genetics.org/cgi/doi/10.1534/genetics.111.135731
698 Cai L, Sutter BM, Li B & Tu BP (2011) Acetyl-CoA induces cell growth and proliferation by
699 promoting the acetylation of histones at growth genes. *Mol. Cell* **42:** 426–37 Available
700 at:
701 http://www.pubmedcentral.nih.gov/articlerender.fcgi?artid=3109073&tool=pmcentrez&
702 rendertype=abstract [Accessed July 30, 2012]
703 Cairns RA, Harris IS & Mak TW (2011) Regulation of cancer cell metabolism. *Nat. Rev.*
704 *Cancer* **11:** 85–95
705 Campbell K, Vowinckel J, Keller MA & Ralser M (2016) Methionine Metabolism Alters
706 Oxidative Stress Resistance via the Pentose Phosphate Pathway. *Antioxid. Redox Signal.*
707 **24:** 543–547
708 Carmona-Saez P, Chagoyen M, Tirado F, Carazo JM & Pascual-Montano A (2007)
709 GENECODIS: a web-based tool for finding significant concurrent annotations in gene
710 lists. *Genome Biol.* **8:** R3
711 Caspi R, Altman T, Billington R, Dreher K, Foerster H, Fulcher CA, Holland TA, Keseler
712 IM, Kothari A, Kubo A, Krummenacker M, Latendresse M, Mueller LA, Ong Q, Paley
713 S, Subhraveti P, Weaver DS, Weerasinghe D, Zhang P & Karp PD (2014) The MetaCyc
714 database of metabolic pathways and enzymes and the BioCyc collection of
715 Pathway/Genome Databases. *Nucleic Acids Res.* **42:** D459-71
716 Cavuoto P & Fenech MF (2012) A review of methionine dependency and the role of
717 methionine restriction in cancer growth control and life-span extension. *Cancer Treat.*
718 *Rev.* **38:** 726–736 Available at: http://dx.doi.org/10.1016/j.ctrv.2012.01.004
719 Cellarier E, Durando X, Vasson MP, Farges MC, Demiden A, Maurizis JC, Madelmont JC &

720 Chollet P (2003) Methionine dependency and cancer treatment. *Cancer Treat. Rev.* **29:**
721 489–99
722 Clarke CJ, Berg TJ, Birch J, Ennis D, Mitchell L, Cloix C, Campbell A, Sumpton D, Nixon
723 C, Campbell K, Bridgeman VL, Vermeulen PB, Foo S, Kostaras E, Jones JL, Haywood
724 L, Pulleine E, Yin H, Strathdee D, Sansom O, et al (2016) The Initiator Methionine
725 tRNA Drives Secretion of Type II Collagen from Stromal Fibroblasts to Promote Tumor
726 Growth and Angiogenesis. *Curr. Biol.* **26:** 755–65
727 Collart MA & Oliviero S (2001) Preparation of Yeast RNA. In *Current Protocols in*
728 *Molecular Biology* Hoboken, NJ, USA: John Wiley & Sons, Inc.
729 Comerford SA, Huang Z, Du X, Wang Y, Cai L, Witkiewicz AK, Walters H, Tantawy MN,
730 Fu A, Manning HC, Horton JD, Hammer RE, Mcknight SL & Tu BP (2014) Article
731 Acetate Dependence of Tumors. *Cell* **159:** 1591–1602 Available at:
732 http://dx.doi.org/10.1016/j.cell.2014.11.020
733 Corbacho I, Teixidó F, Velázquez R, Hernández LM & Olivero I (2011) Standard YPD, even
734 supplemented with extra nutrients, does not always compensate growth defects of
735 Saccharomyces cerevisiae auxotrophic strains. *Antonie Van Leeuwenhoek* **99:** 591–600
736 DeBerardinis RJ, Sayed N, Ditsworth D & Thompson CB (2008) Brick by brick: metabolism
737 and tumor cell growth. *Curr. Opin. Genet. Dev.* **18:** 54–61
738 Dechant R & Peter M (2008) Nutrient signals driving cell growth. *Curr. Opin. Cell Biol.* **20:**
739 678–87 Available at: http://www.ncbi.nlm.nih.gov/pubmed/18930818 [Accessed July
740 25, 2012]
741 van Dijken JP, Bauer, Brambilla, Duboc, Francois, Gancedo, Giuseppin, Heijnen, Hoare,
742 Lange, Madden, Niederberger, Nielsen, Parrou, Petit, Porro, Reuss, van Riel N, Rizzi,
743 Steensma, et al (2000) An interlaboratory comparison of physiological and genetic
744 properties of four Saccharomyces cerevisiae strains. *Enzyme Microb. Technol.* **26:** 706–

714

Doherty D (1970) [119] l-glutamate dehydrogenases (yeast). In pp 850–856.

Dong Y-X, Sueda S, Nikawa J-I & Kondo H (2004) Characterization of the products of the genes SNO1 and SNZ1 involved in pyridoxine synthesis in Saccharomyces cerevisiae. *Eur. J. Biochem.* **271:** 745–752

Dwight SS, Harris MA, Dolinski K, Ball CA, Binkley G, Christie KR, Fisk DG, Issel-Tarver L, Schroeder M, Sherlock G, Sethuraman A, Weng S, Botstein D & Cherry JM (2002) Saccharomyces Genome Database (SGD) provides secondary gene annotation using the Gene Ontology (GO). *Nucleic Acids Res.* **30:** 69–72

Eliot AC & Kirsch JF (2004) Pyridoxal phosphate enzymes: mechanistic, structural, and evolutionary considerations. *Annu. Rev. Biochem.* **73:** 383–415

Faubert B, Li KY, Cai L, Hensley CT, Kim J, Zacharias LG, Yang C, Do QN, Doucette S, Burguete D, Li H, Huet G, Yuan Q, Wigal T, Butt Y, Ni M, Torrealba J, Oliver D, Lenkinski RE, Malloy CR, et al (2017) Lactate Metabolism in Human Lung Tumors. *Cell* **171:** 358–371.e9

Gerashchenko M V. & Gladyshev VN (2014) Translation inhibitors cause abnormalities in ribosome profiling experiments. *Nucleic Acids Res.* **42:** e134–e134

González A & Hall MN (2017) Nutrient sensing and TOR signaling in yeast and mammals. *EMBO J.* **8:** e201696010 Available at: http://emboj.embopress.org/lookup/doi/10.15252/embj.201696010

Gray J V., Petsko GA, Johnston GC, Ringe D, Singer RA & Werner-Washburne M (2004) 'Sleeping beauty': quiescence in Saccharomyces cerevisiae. *Microbiol. Mol. Biol. Rev.* **68:** 187–206

Gu X, Orozco JM, Saxton RA, Condon KJ, Liu GY, Krawczyk PA, Scaria SM, Harper JW, Gygi SP & Sabatini DM (2017) SAMTOR is an S -adenosylmethionine sensor for the

770 mTORC1 pathway. *Science (80-.).* **818:** 813–818

771 Guo HY, Herrera H, Groce A & Hoffman RM (1993) Expression of the biochemical defect
772 of methionine dependence in fresh patient tumors in primary histoculture. *Cancer Res.*
773 **53:** 2479–83

774 Halpern BC, Clark BR, Hardy DN, Halpern RM & Smith RA (1974) The effect of
775 replacement of methionine by homocystine on survival of malignant and normal adult
776 mammalian cells in culture. *Proc. Natl. Acad. Sci. U. S. A.* **71:** 1133–6

777 Heiden MG Vander, Cantley LC & Thompson CB (2009) Understanding the Warburg Effect:
778 The Metabolic Requirements of Cell Proliferation. *Science (80-.).* **324:** 1029–1033

779 Hinnebusch AG (2005) Translational regulation of GCN4 and the general amino acid control
780 of yeast. *Annu. Rev. Microbiol.* **59:** 407–50

781 Hu X, Chao M & Wu H (2017) Central role of lactate and proton in cancer cell resistance to
782 glucose deprivation and its clinical translation. *Signal Transduct. Target. Ther.* **2:** 16047

783 Jorgensen P & Tyers M (2004) How Cells Coordinate Growth and Division. *Curr. Biol.* **14:**
784 R1014–R1027 Available at:
785 http://linkinghub.elsevier.com/retrieve/pii/S0960982204008954

786 Kaleta C & Schäuble S (2013) Metabolic costs of amino acid and protein production in
787 Escherichia coli. *Biotechnol. J.* **8:** 1105–1114 Available at:
788 http://onlinelibrary.wiley.com/doi/10.1002/biot.201200267/abstract

789 Kennedy KM, Scarbrough PM, Ribeiro A, Richardson R, Yuan H, Sonveaux P, Landon CD,
790 Chi J-T, Pizzo S, Schroeder T & Dewhirst MW (2013) Catabolism of exogenous lactate
791 reveals it as a legitimate metabolic substrate in breast cancer. *PLoS One* **8:** e75154

792 Klosinska MM, Crutchfield CA, Bradley PH, Rabinowitz JD & Broach JR (2011) Yeast cells
793 can access distinct quiescent states. *Genes Dev.* **25:** 336–49 Available at:
794 http://www.pubmedcentral.nih.gov/articlerender.fcgi?artid=3042157&tool=pmcentrez&

795 rendertype=abstract
796 Kokkinakis DM, Hoffman RM, Frenkel EP, Wick JB, Han Q, Xu M, Tan Y & Schold SC
797 (2001) Synergy between methionine stress and chemotherapy in the treatment of brain
798 tumor xenografts in athymic mice. *Cancer Res.* **61:** 4017–23
799 Lagniel G, Aude J, Lombardia L, Soularue P, Petat C, Werner M, Labarre J, Evry CEA &
800 Cre G (2002) Sulfur Sparing in the Yeast Proteome in Response to Sulfur Demand Mire.
801 *Mol. Cell* **9:** 713–723
802 Laxman S, Sutter BMBM, Shi L & Tu BPBP (2014a) Npr2 inhibits TORC1 to prevent
803 inappropriate utilization of glutamine for biosynthesis of nitrogen-containing
804 metabolites. *Sci. Signal.* **7:** ra120
805 Laxman S, Sutter BMBM & Tu BPBP (2014b) Methionine is a signal of amino acid
806 sufficiency that inhibits autophagy through the methylation of PP2A. *Autophagy* **10:**
807 386–387
808 Laxman S, Sutter BMBM, Wu XX, Kumar S, Guo X, Trudgian DCDC, Mirzaei H & Tu
809 BPBP (2013) Sulfur Amino Acids Regulate Translational Capacity and Metabolic
810 Homeostasis through Modulation of tRNA Thiolation. *Cell* **154:** 416–429 Available at:
811 http://linkinghub.elsevier.com/retrieve/pii/S0092867413008258
812 Laxman S & Tu BP (2010) Systems approaches for the study of metabolic cycles in yeast.
813 *Curr. Opin. Genet. Dev.* **20:** 599–604 Available at:
814 http://www.pubmedcentral.nih.gov/articlerender.fcgi?artid=3138152&tool=pmcentrez&
815 rendertype=abstract [Accessed August 31, 2012]
816 Lee BC, Kaya A & Gladyshev VN (2016) Methionine restriction and life-span control. *Ann.*
817 *N. Y. Acad. Sci.* **1363:** 116–124
818 Lee BC, Kaya A, Ma S, Kim G, Gerashchenko M V., Yim SH, Hu Z, Harshman LG &
819 Gladyshev VN (2014) Methionine restriction extends lifespan of Drosophila

820 melanogaster under conditions of low amino-acid status. *Nat. Commun.* **5:**
821 Li H & Durbin R (2009) Fast and accurate short read alignment with Burrows-Wheeler
822 transform. *Bioinformatics* **25:** 1754–1760
823 Ljungdahl PO & Daignan-Fornier B (2012) Regulation of Amino Acid, Nucleotide, and
824 Phosphate Metabolism in Saccharomyces cerevisiae. *Genetics* **190:** 885–929 Available
825 at: http://www.genetics.org/cgi/doi/10.1534/genetics.111.133306
826 Lu S & Epner DE (2000) Molecular mechanisms of cell cycle block by methionine restriction
827 in human prostate cancer cells. *Nutr. Cancer* **38:** 123–30
828 Mampel J, Schröder H, Haefner S & Sauer U (2005) Single-gene knockout of a novel
829 regulatory element confers ethionine resistance and elevates methionine production in
830 Corynebacterium glutamicum. *Appl. Microbiol. Biotechnol.* **68:** 228–36
831 Mariño G, Pietrocola F, Eisenberg T, Kong Y, Malik SA, Andryushkova A, Schroeder S,
832 Pendl T, Harger A, Niso-Santano M, Zamzami N, Scoazec M, Durand S, Enot DP,
833 Fernández ÁF, Martins I, Kepp O, Senovilla L, Bauvy C, Morselli E, et al (2014)
834 Regulation of autophagy by cytosolic acetyl-coenzyme A. *Mol. Cell* **53:** 710–25
835 Mulleder M, Calvani E, Alam MT, Wang RK, Eckerstorfer F, Zelezniak A & Ralser M
836 (2016) Functional Metabolomics Describes the Yeast Biosynthetic Regulome. *Cell* **167:**
837 553–565.e12
838 Natarajan K, Meyer MR, Jackson BM, Slade D, Roberts C, Hinnebusch AG & Marton MJ
839 (2001) Transcriptional profiling shows that Gcn4p is a master regulator of gene
840 expression during amino acid starvation in yeast. *Mol. Cell. Biol.* **21:** 4347–68
841 Nelson, DL; Cox M (2017) Principles of biochemistry 7th ed. NY, USA: W. H. Freeman
842 Nogales-Cadenas R, Carmona-Saez P, Vazquez M, Vicente C, Yang X, Tirado F, Carazo JM
843 & Pascual-Montano A (2009) GeneCodis: interpreting gene lists through enrichment
844 analysis and integration of diverse biological information. *Nucleic Acids Res.* **37:**

845 W317–W322
846 Palam LR, Gore J, Craven KE, Wilson JL & Korc M (2015) Integrated stress response is
847 critical for gemcitabine resistance in pancreatic ductal adenocarcinoma. *Cell Death Dis.*
848 **6:** e1913
849 Patra KC & Hay N (2014) The pentose phosphate pathway and cancer. *Trends Biochem. Sci.*
850 **39:** 347–354 Available at: http://dx.doi.org/10.1016/j.tibs.2014.06.005
851 Pedro MB & Madeo F (2015) Review Acetyl Coenzyme A : A Central Metabolite and
852 Second Messenger. *Cell Metab.* **21:** 805–821
853 Poirson-Bichat F, Gonçalves RA, Miccoli L, Dutrillaux B & Poupon MF (2000) Methionine
854 depletion enhances the antitumoral efficacy of cytotoxic agents in drug-resistant human
855 tumor xenografts. *Clin. Cancer Res.* **6:** 643–53
856 Pronk JT (2002) Auxotrophic yeast strains in fundamental and applied research. *Appl.*
857 *Environ. Microbiol.* **68:** 2095–100
858 Robinson MD, McCarthy DJ & Smyth GK (2010) edgeR: a Bioconductor package for
859 differential expression analysis of digital gene expression data. *Bioinformatics* **26:** 139–
860 40
861 Sherman F (1991) Getting started with yeast. *Methods Enzymol.* **194:** 3–21
862 Shi L & Tu BP (2013) Acetyl-CoA induces transcription of the key G1 cyclin CLN3 to
863 promote entry into the cell division cycle in Saccharomyces cerevisiae. *Proc. Natl.*
864 *Acad. Sci.* **110:** 7318–7323
865 Slavov N & Botstein D (2011) Coupling among growth rate response, metabolic cycle, and
866 cell division cycle in yeast. *Mol. Biol. Cell* **22:** 1997–2009 Available at:
867 http://www.molbiolcell.org/content/22/12/1997.full
868 Slavov N & Botstein D (2013) Decoupling nutrient signaling from growth rate causes aerobic
869 glycolysis and deregulation of cell size and gene expression. *Mol. Biol. Cell* **24:** 157–

870 168 Available at: http://www.molbiolcell.org/cgi/doi/10.1091/mbc.E12-09-0670
871 Srinivasan R, Chandraprakash D, Krishnamurthi R, Singh P, Scolari VF, Krishna S &
872 Seshasayee ASN (2013) Genomic analysis reveals epistatic silencing of 'expensive'
873 genes in Escherichia coli K-12. *Mol. Biosyst.* **9:** 2021–33
874 Stern PH & Hoffman RM (1986) Enhanced in vitro selective toxicity of chemotherapeutic
875 agents for human cancer cells based on a metabolic defect. *J. Natl. Cancer Inst.* **76:**
876 629–39
877 Sugimura T, Birnbaum SM, Winitz M & Greenstein JP (1959) Quantitative nutritional
878 studies with water-soluble, chemically defined diets. VIII. The forced feeding of diets
879 each lacking in one essential amino acid. *Arch. Biochem. Biophys.* **81:** 448–455
880 Sutter BMBM, Wu XX, Laxman S & Tu BPBP (2013) Methionine inhibits autophagy and
881 promotes growth by inducing the SAM-responsive methylation of PP2A. *Cell* **154:** 403–
882 15
883 Tabas-Madrid D, Nogales-Cadenas R & Pascual-Montano A (2012) GeneCodis3: a non-
884 redundant and modular enrichment analysis tool for functional genomics. *Nucleic Acids*
885 *Res.* **40:** W478–W483
886 Thomas D, Cherest H & Surdin-Kerjan Y (1991) Identification of the structural gene for
887 glucose-6-phosphate dehydrogenase in yeast. Inactivation leads to a nutritional
888 requirement for organic sulfur. *EMBO J.* **10:** 547–53
889 Thomas D, Surdin-kerjan Y & Ge C De (1997) Metabolism of Sulfur Amino Acids in
890 Saccharomyces cerevisiae. *Microbiol. Mol. Biol. Rev.* **61:** 503–532
891 Tong X, Zhao F & Thompson CB (2009) The molecular determinants of de novo nucleotide
892 biosynthesis in cancer cells. *Curr. Opin. Genet. Dev.* **19:** 32–7
893 Troen AM, French EE, Roberts JF, Selhub J, Ordovas JM, Parnell LD & Lai C-Q (2007)
894 Lifespan modification by glucose and methionine in Drosophila melanogaster fed a

895 chemically defined diet. *Age (Dordr).* **29:** 29–39

896 Tu BP, Kudlicki A, Rowicka M & McKnight SL (2005) Logic of the yeast metabolic cycle:
897 temporal compartmentalization of cellular processes. *Science* **310:** 1152–1158

898 Tu BP, Mohler RE, Liu JC, Dombek KM, Young ET, Synovec RE & McKnight SL (2007)
899 Cyclic changes in metabolic state during the life of a yeast cell. *Proc. Natl. Acad. Sci. U.*
900 *S. A.* **104:** 16886–16891

901 Unger MW & Hartwell LH (1976) Control of cell division in Saccharomyces cerevisiae by
902 methionyl-tRNA. *Proc. Natl. Acad. Sci. U. S. A.* **73:** 1664–8 Available at:
903 http://www.pubmedcentral.nih.gov/articlerender.fcgi?artid=430360&tool=pmcentrez&r
904 endertype=abstract

905 Vattem KM & Wek RC (2004) Reinitiation involving upstream ORFs regulates ATF4
906 mRNA translation in mammalian cells. *Proc. Natl. Acad. Sci. U. S. A.* **101:** 11269–74

907 Warburg O (1956) On the origin of cancer cells. *Science* **123:** 309–14

908 Warner JR (1999) The economics of ribosome biosynthesis in yeast. *Trends Biochem. Sci.*
909 **24:** 437–40 Available at: http://www.ncbi.nlm.nih.gov/pubmed/10542411

910 Warner JR, Vilardell J & Sohn JH (2001) Economics of ribosome biosynthesis. *Cold Spring*
911 *Harb. Symp. Quant. Biol.* **66:** 567–74

912 Wolfson RL & Sabatini DM (2017) The Dawn of the Age of Amino Acid Sensors for the
913 mTORC1 Pathway. *Cell Metab.* **26:** 301–309

914 Wu X & Tu BP (2011) Selective regulation of autophagy by the Iml1-Npr2-Npr3 complex in
915 the absence of nitrogen starvation. *Mol. Biol. Cell* **22:** 4124–4133 Available at:
916 http://www.molbiolcell.org/cgi/content/abstract/22/21/4124%5Cnpapers2://publication/d
917 oi/10.1091/mbc.E11-06-0525

918 Xu Y-F, Létisse F, Absalan F, Lu W, Kuznetsova E, Brown G, Caudy A a, Yakunin AF,
919 Broach JR & Rabinowitz JD (2013) Nucleotide degradation and ribose salvage in yeast.

920 *Mol. Syst. Biol.* **9:** 665 Available at: http://msb.embopress.org/content/9/1/665.abstract

921 Ye C, Sutter BM, Wang Y, Kuang Z & Tu BP (2017) A Metabolic Function for Phospholipid
922 and Histone Methylation. *Mol. Cell* **66:** 180–193.e8

923 Ye J, Kumanova M, Hart LS, Sloane K, Zhang H, De Panis DN, Bobrovnikova-Marjon E,
924 Diehl JA, Ron D & Koumenis C (2010) The GCN2-ATF4 pathway is critical for tumour
925 cell survival and proliferation in response to nutrient deprivation. *EMBO J.* **29:** 2082–96

926

927

928